



## Invited review

# Onshore to offshore anatomy of a late Quaternary source-to-sink system (Po Plain–Adriatic Sea, Italy)

Alessandro Amorosi <sup>a</sup>, Vittorio Maselli <sup>b</sup>, Fabio Trincardi <sup>b</sup><sup>a</sup> Dipartimento di Scienze Biologiche, Geologiche e Ambientali, University of Bologna, Via Zamboni 67, 40126 Bologna, Italy<sup>b</sup> Istituto di Scienze Marine (ISMAR-CNR), Via Gobetti 101, 40129 Bologna, Italy

## ARTICLE INFO

## Article history:

Received 13 September 2014

Received in revised form 22 October 2015

Accepted 27 October 2015

Available online 28 October 2015

## Keywords:

Source-to-sink analysis  
Sequence stratigraphy  
Sediment budget  
Late Quaternary  
Po Plain  
Adriatic Sea  
Italy

## ABSTRACT

In understanding the evolution of siliciclastic systems, Late Quaternary analogs may enable reliable predictive models of facies-tract architecture. The Po Plain–Adriatic Sea system, where a wealth of research has been conducted during the last 20 years, represents one of the most intensively investigated late Quaternary successions. With the aid of a chronologically well-constrained stratigraphy, paleoenvironmental evolution is tracked for the first time from fluvial to deep-marine realms, over 1000 km in length. Vertical stacking trends (onshore) and stratal terminations (offshore) are the key observations that allow identification of surfaces with sequence-stratigraphic significance (systems tract boundaries) in the distinct segments of the system. Recurring motifs in stratigraphic architecture, showing tight coupling of sedimentary responses among source area, catchment basin, and coastal and marine depocenters, reveal a cyclicity driven by glacio-eustatic fluctuations in the Milankovitch band. Due to high rates of subsidence, middle Pleistocene forced regressive systems tracts are exceptionally expanded, and the MIS5e–MIS2 interval (Late Pleistocene) preserves a nearly continuous record of fourth-order (100 kyr) stepwise sea-level fall. The stratigraphic architecture of Last Glacial Maximum deposits highlights the genetic relations between channel-belt development, pedogenesis, and sediment delivery to the lowstand delta, through narrow incised-valley conduits. The Late glacial-Holocene succession records the last episode of sea-level rise and stabilization through well-developed patterns of shoreline transgression/regression (TST/HST) that can be readily traced updip, from offshore to onshore locations. Architectural styles across the whole system reflect a dominance of allogenic forcing in the TST, as opposed to a predominantly autogenic control on stratigraphic development in the HST. External drivers of facies architecture were also effective on millennial timescales: the Younger Dryas cold reversal, which marks the transgressive surface on land, records a short-lived episode of subaqueous progradation that is correlative onshore with widespread, immature paleosol development and small-sized channel-belt formation. Quantitative assessment of sediment budgets over different time intervals requires precise positioning of the key bounding surfaces. Based on this approach, we outline for the first time over the entire Po–Adriatic Basin an estimate of the sediment volumes stored in each systems tract.

© 2015 Elsevier B.V. All rights reserved.

## Contents

1. Introduction . . . . .	213
2. Geological setting . . . . .	214
2.1. Overview . . . . .	214
2.2. Tectonic setting . . . . .	215
2.3. Oceanographic setting . . . . .	215
2.4. Sediment flux to the Adriatic Basin . . . . .	215
3. Middle-late Pleistocene record of Milankovitch-scale cyclicity . . . . .	216
3.1. Onshore stratigraphy . . . . .	216
3.2. Offshore stratigraphy . . . . .	217
4. Data and methods . . . . .	217
5. Forced regressive systems tract (~115–30 cal kyr BP) . . . . .	218

E-mail address: [alessandro.amorosi@unibo.it](mailto:alessandro.amorosi@unibo.it) (A. Amorosi).

5.1. Onshore stratigraphy . . . . .	218
5.2. Offshore stratigraphy . . . . .	219
6. Lowstand systems tract (~30–18 cal kyr BP) . . . . .	220
6.1. Onshore stratigraphy . . . . .	220
6.2. Offshore stratigraphy . . . . .	222
7. Transgressive systems tract (18–6 cal kyr BP) . . . . .	223
7.1. Onshore stratigraphy . . . . .	223
7.2. Offshore stratigraphy . . . . .	225
8. Highstand systems tract (6 cal kyr BP to Present) . . . . .	226
8.1. Onshore stratigraphy . . . . .	226
8.2. Offshore stratigraphy . . . . .	227
9. The Po Plain–Adriatic system: a source-to-sink approach . . . . .	229
9.1. Key stratigraphic surfaces . . . . .	229
9.2. Paleoenvironmental evolution . . . . .	230
10. Sediment budget . . . . .	231
10.1. Approach . . . . .	231
10.2. Systems tract volumes and sediment budget partitioning . . . . .	231
10.3. Human impact on sediment budgets . . . . .	233
11. Conclusions . . . . .	233
Acknowledgments . . . . .	234
References . . . . .	234

## 1. Introduction

Deciphering the mechanisms that regulate sediment production, transfer and storage in a source-to-sink perspective and its integration with sequence stratigraphic concepts may significantly help in understanding and predicting the stratigraphic architecture of clastic depositional systems (Blum and Womack, 2009; Catuneanu et al., 2009). In a source-to-sink view, erosional and depositional landscapes are linked by the sediment-routing system (Allen, 2008), and genetically related morphodynamic sectors can be viewed as distinct segments of the dispersal system (Sømme et al., 2009, 2011; Martinsen et al., 2010; Paola and Leeder, 2011).

One of the aims of source-to-sink analysis is to extract quantitative sediment flux data that can be integrated with stratigraphic models for estimating sediment budgets from ancient successions. Sediment flux to the coastal zone, and down to the deep basin, is conditioned by a variety of factors, including geomorphic and tectonic influences, climate, geology, and human activities (Svitski and Milliman, 2007). When attempting to reconstruct sediment budgets from the ancient record, scaling relationships derived from modern systems may serve to quantify unknown factors having knowledge of the others (Blum et al., 2013; Sømme and Jackson, 2013).

Owing to (i) limited stratigraphic resolution, (ii) tectonic disturbance, and commonly (iii) poor chronologic control, source-to-sink analysis can hardly be tested in ancient successions. In contrast, modern systems, where deposits and forcing mechanisms can be independently dated and mapped, represent archives where process controls can be thoroughly interrogated and, at least in part, quantified (Blum et al., 2013). In this context, robust models of relationships between stratigraphic architecture and sea-level or climate change can be built up for late Quaternary or Holocene successions much better than for any other period in Earth history.

Quaternary sedimentary successions have long represented one of the key testing grounds for sequence stratigraphic models (Dalrymple et al., 1994; Blum and Törnqvist, 2000; Boyd et al., 2006; Blum et al., 2013), and the most comprehensive source-to-sink studies rely upon recent continental margins, including the Fly/Strickland rivers-Gulf of Papua system (Walsh et al., 2004; Swenson et al., 2005; Slingerland et al., 2008; Lauer et al., 2008; Walsh and Ridd, 2009) and the Waipaoa River system on the East coast of New Zealand's North Island (Alexander et al., 2010; Carter et al., 2010; Gerber et al., 2010). In order to investigate the sedimentary response to fluctuations in sea level, climate, and tectonics from catchment to deep basin, source-to-sink analysis

has focused on comparatively small-sized systems, encompassing preferably short and steep rivers (Sømme et al., 2009). In Europe, well-known examples are from the Norwegian continental margin (Martinsen et al., 2010; Sømme and Jackson, 2013) and the Golo River system in NE Corsica, France (Sømme et al., 2011; Calvès et al., 2013). A comprehensive assessment of land-to-deep-sea sediment budgets over millennia with significant climate change (glacial to interglacial transitions) is almost lacking (Covault et al., 2011).

The Po Plain–Adriatic Sea system, within the Alpine–Apennine foreland basin (Fig. 1), is a peculiar setting, influenced by high and laterally variable subsidence and sediment supply rates under rapid high-magnitude relative sea-level change. A high amount of high-resolution, sequence stratigraphic research has been carried out over the past two decades, both offshore (Trincardi et al., 1994, 1996; Cattaneo and Trincardi, 1999; Trincardi and Corregiari, 2000; Ridente and Trincardi, 2002, 2005, 2006; Ridente et al., 2008, 2009; Maselli et al., 2010, 2011; Maselli and Trincardi, 2013a) and onshore (Amorosi et al., 1999a,b, 2003, 2004, 2005, 2008a,b, 2014; Scarponi and Kowalewski, 2004; Scarponi et al., 2013). In this regional context, and based on well-constrained physical correlations, process-observing research has shed light on strata formation from flood events from the Po and Apennine rivers within the EUROSTRATAFORM project (Nittrouer et al., 2004).

Beneath the Po Plain regional subsidence exhibits high values, of about 1 mm/yr over the last 800 kyr. Owing to such high subsidence rates, forced-regressive deposits of late Pleistocene (post-MIS5e) age are exceptionally well preserved, with thicknesses up to 100 m (Amorosi et al., 2004). Similarly, tectonic subsidence enhanced accumulation and preservation of the 350-m-thick lowstand Po Delta, in the shelf area north of the Mid Adriatic Deep (MAD in Fig. 1), along with a set of mud-prone regressive sequences recording the last four 100-kyr climate-driven sea-level cycles, south of the MAD (Trincardi and Corregiari, 2000). The refined chronological framework available for these Quaternary successions makes it possible to investigate the interaction between fluvio-deltaic, shelf and deep-marine processes under conditions of very rapidly fluctuating sea level and sediment supply, both at the Milankovitch (100 to 20 kyr) and sub-Milankovitch (millennial to centennial) time scales.

The Po Plain–Adriatic Sea system thus represents a uniquely suited natural laboratory, where complementary offshore and onshore research provides a modern analog of source-to-sink analysis, with remarkable implications for hydrocarbon exploration. Through a summary of detailed middle Pleistocene to Recent sequence stratigraphy,

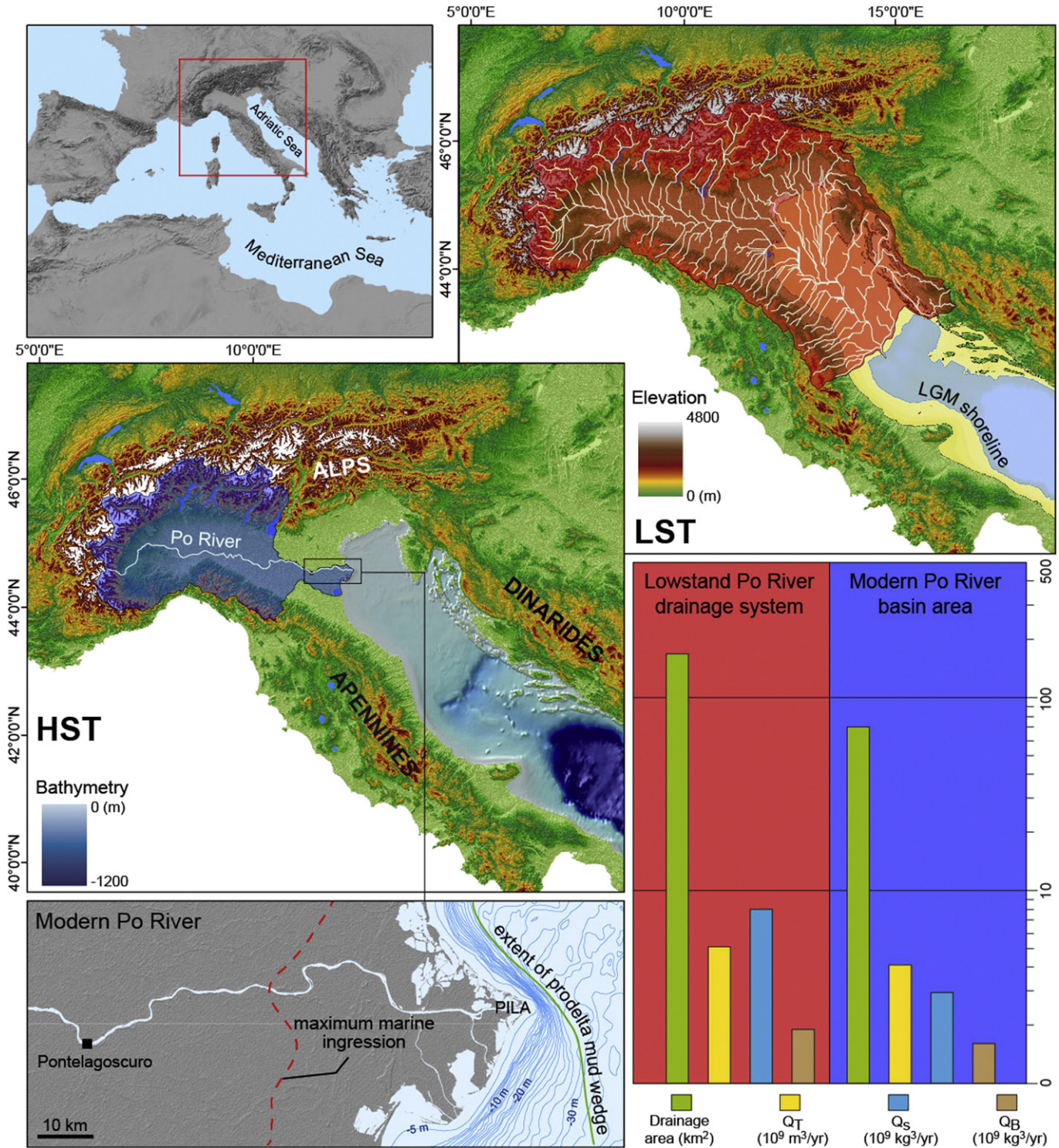


**Fig. 1.** The Po Plain–Adriatic system at present (HST), central left, and its physiography reconstructed at time of maximum marine regression (LST), upper right, with inferred drainage directions, drainage areas and sediment discharge (from Maselli et al., 2011).  $Q_T$ : total sediment discharge;  $Q_S$ : suspended-load discharge;  $Q_B$ : bed-load discharge.

specific objectives of this paper are (i) to illustrate facies distribution and stratigraphic preservation from the Po River catchment to the deep Adriatic Sea; (ii) to test the sequence stratigraphic approach through a chronologically well-constrained example from alluvial plain to continental slope domains forced by both local (i.e. autogenic) and regional-to-global (i.e. allogenic) factors; (iii) to define the impact of Milankovitch to sub-Milankovitch scale climate change on systems tract architecture within the late-Quaternary depositional sequence (MIS5e to MIS1); and (iv) to make a first quantitative assessment of

sediment budgets for the Po Plain–Adriatic basin on a systems tract scale.

## 2. Geological setting

### 2.1. Overview

The Po Plain–Adriatic Sea system is part of the Alpine–Apennine and Dinarides–Hellenides foreland, an elongated basin largely filled from

the Po River catchment located in the North (Fig. 1). The Po Plain, one of the widest European alluvial plains ( $74,500 \text{ km}^2$ ), is a densely populated area that hosts about one third of the Italian population. The Po River, the longest river in Italy (652 km), flows from West to East with the largest sediment discharge into the Adriatic Sea. The northern Apennines and the southern Alps are drained toward the Po by numerous parallel rivers, and the axial Po fluvial system is oriented sub-parallel to the Apennines thrust front. The Adriatic Sea is a narrow semi-enclosed basin (roughly  $200 \text{ km} \times 800 \text{ km}$ ) elongated in NW–SE direction and surrounded by three mountain belts: the Alps, in the North, the Apennines, W and SW, and the Dinarides on the East.

The modern structural setting of the Po Plain and of the western Adriatic margin reflects the Meso-Cenozoic subduction of the Adriatic plate and the accretion of the Apennine chain (Doglioni, 1993), which induced a combined effect of (i) thrust loading, (ii) westward tilting of the Adriatic margin along the thrust front, and (iii) asymmetric sediment flux with clear dominance of sources from the W and SW, where uplift and erosion of older deposits were greatest. After an earlier phase dominated by basin-floor turbidite sedimentation, during the Quaternary the Adriatic basin became increasingly dominated by progradational deposits advancing from the Po Plain along the major axis of the basin, NW–SE (Ori et al., 1986). This change in depositional style reflects, primarily, an interval of decreased uplift and reduced eastward migration of the Apennine front and allows this basin, as a whole, potentially to record all Milankovitch types of cyclicity and related unconformities.

Today the shelf break is about 300 km away from the northern Adriatic coast and the shelf presents a gentle dip of about  $0.02^\circ$  toward the SE. The MAD (Fig. 1), South of the shelf break, represents a small slope basin with maximum depth of 260 m, which has been progressively filled from the NW by the Po River delta during repeated Quaternary phases of sea-level fall and lowstand (Ciabatti et al., 1987; Dalla Valle et al., 2013a,b). The last progradational wedge originated during the Last Glacial Maximum or LGM (Trincardi et al., 1996; Cattaneo and Trincardi, 1999; Asioli et al., 2001). In the Central Adriatic the continental shelf extends seaward about 50 km parallel to the front of the Apennine chain, with a more pronounced seafloor dip of  $0.3^\circ$ – $0.7^\circ$ . The South Adriatic is a deeper basin showing complex slope morphology and maximum depth of about 1200 m (Fig. 1). The Mid Adriatic Deep and the South Adriatic Basin are connected through the Pelagruza Sill, a few tens of km wide and reaching a depth of 180 m (Trincardi et al., 2014).

## 2.2. Tectonic setting

The westward subduction of the Adria plate, a promontory of the African plate, in the context of the convergence between the European and African plates, during the last 25 Ma led to the formation of the Apennine chain. At that time, the Po Plain–Adriatic basin became a foreland domain where thick syn-orogenic clastic sequences were deposited (Doglioni, 1993). During the Pliocene and Pleistocene, the Po Plain and the Central Adriatic basin were affected by high subsidence rates because of the eastward rollback of the Apennine subduction hinge (Royden et al., 1987). Due to the fast subsidence induced by the tectonic loading of the two chains, the more external fronts of the Alpine and Apennine thrust belts were buried beneath the Po Plain (Burrato et al., 2003) and the Central Adriatic (Maselli et al., 2010). The Adriatic foredeep, south of Gargano Promontory has been, in contrast, characterized by uplift since the Middle Pleistocene (Doglioni et al., 1994; Scrocca, 2006; Ridente and Trincardi, 2006). This different tectonic behavior has been ascribed to differences in thickness of the west-directed subduction of the Adriatic lithosphere (Pieri and Groppi, 1981; Royden et al., 1987; Doglioni et al., 1994).

Diffuse folding and thrusting have been imaged in the subsurface of the Po Plain by geophysical studies (Pieri and Groppi, 1981). In particular, the North Apennine frontal thrust system, buried below the southern margin of the Po Plain (Ferrara and Emilia arcs) makes this

area seismically active, as confirmed by the M 6.0 earthquake of 2012 (Caputo et al., 2012). Because of its active structural framework, the Pliocene–Quaternary Po Basin fill shows comparatively reduced thickness (about 100 m) in ramp anticline zones, whereas it may exceed 7000 m in the thickest depocenters (Pieri and Groppi, 1981; Doglioni, 1993; Regione Emilia-Romagna and Eni-Agip, 1998; Carminati et al., 2003 – Fig. 2A). In the Mirandola anticline, one of the fastest growing structures of the whole Apennines, vertical displacement rates of up to  $1.7 \text{ mm/yr}$  have been calculated (Burrato et al., 2003; Carminati and Vadacca, 2010).

The sedimentary record of the Po Basin is asymmetric, with a depocenter shifted toward the Apennines filling a wedge-shaped basin with the deep part of the wedge adjacent to the thrust front (Regione Emilia-Romagna and Eni-Agip, 1998; Picotti and Pazzaglia, 2008). The basin fill records an overall “regressive” trend, from deep-marine to continental deposits (Ricci Lucchi et al., 1982). Stratigraphic geometries, visible in seismic lines, clearly show that the degree of tectonic deformation progressively decreases from the oldest (Pliocene) to the youngest (late Quaternary) units (Fig. 2A).

## 2.3. Oceanographic setting

The Adriatic basin displays a general counter-clockwise circulation pattern driven by wind forcing and freshwater input from the Po and Apennine rivers ( $Q_w$  is about  $5700 \text{ m}^3 \text{ s}^{-1}$  on average). Altogether, three main water masses impact the Adriatic Sea: (i) the Levantine Intermediate Water (LIW), flowing in from the eastern Mediterranean through the Otranto Strait; (ii) the North Adriatic Dense Water (NAdDW), forming in the Northern Adriatic shelf during cold wind outbreaks in late winter (Bergamasco et al., 1999; Vilibić, 2003; Benetazzo et al., 2014; Chiggiato et al., 2015; Carniel et al., 2015); and (iii) the South Adriatic Dense Water (SADW), forming through a mechanism of open-ocean convection in the southern Adriatic deep. The NAdDW, in particular, is a very dense water mass that flows south as an underflow vein along the isobaths (Artegiani and Salusti, 1987; Artegiani et al., 1997; Vilibić and Supić, 2005; Querin et al., 2013) at a depth of 50–150 m, impinging the western rim of the MAD (Jabuka pit in Fig. 1; Marini et al., 2015); past the Gargano Promontory the NAdDW sinks into deeper waters, extensively impacting the sea-floor morphology (Verdicchio and Trincardi, 2006; Trincardi et al., 2007a,b). The SADW is the result of the permanent South Adriatic cyclonic gyre, and interacts with the LIW and NAdDW as it flows through the Otranto Strait, the bottleneck connection to the eastern Mediterranean.

In response to these intense cooling episodes, the heat fluxes from the ocean to the atmosphere can reach values up to  $1000 \text{ W/m}^2$  (Supić and Orlić, 1999; Boldrin et al., 2009) and waters present a potential density anomaly exceeding  $29.6 \text{ kg m}^{-3}$  (Bergamasco et al., 1999; Vilibić and Supić, 2005), up to  $30.0 \text{ kg m}^{-3}$  (Supić and Orlić, 1999). The dense waters tend to flow along topographic features as a quasi-geostrophic flow (Benetazzo et al., 2014) and are responsible for sediment redistribution along the Italian coast, as documented by Cattaneo et al. (2003, 2007).

## 2.4. Sediment flux to the Adriatic Basin

In its northernmost portion, this marginal semi-enclosed basin within the northern Mediterranean constitutes a shallow continental shelf with depths on the order of a few tens of meters, occasionally exposed to intense winds. In this area, the Po discharges its freshwater at a rate of  $1500 \text{ m}^3 \text{ s}^{-1}$  (yearly averaged value, Nelson, 1970; Falcieri et al., 2013). Fluvial sediment sources are located dominantly along the western side of the Adriatic Basin, with combined modern delivery of  $51.7 \times 10^6 \text{ tons yr}^{-1}$  of mean suspended load. The sediment yield from the Dinarides is negligible because of the intensely fractured and karstic nature of the catchments, trapping water flows and sediment in basins close to the coastal area. The contribution from the eastern Alpine rivers is  $3 \times 10^6 \text{ tons yr}^{-1}$ , from the Po is  $15 \times 10^6 \text{ tons yr}^{-1}$ ,

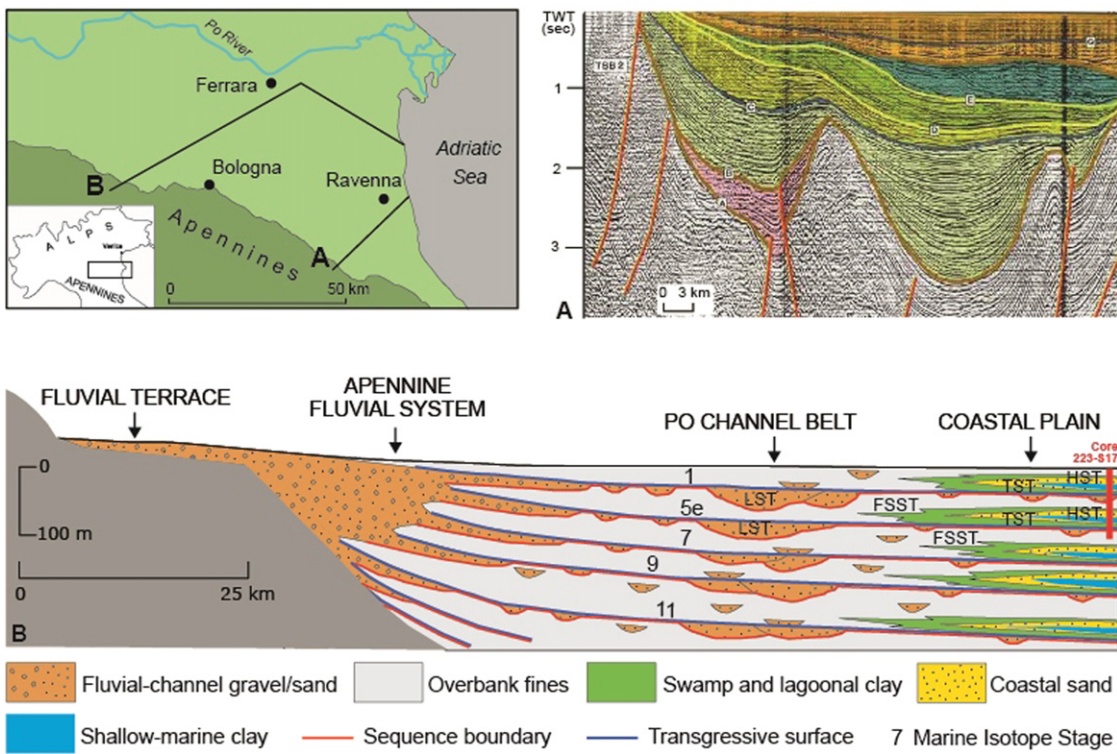


**Fig. 2.** A: Seismic profile showing the Pliocene-Quaternary Po Basin fill and its subdivision into third-order depositional sequences (colored units – from [Regione Emilia-Romagna and Eni-Agip, 1998](#)). B: Fourth-order transgressive-regressive sequences formed in response to Milankovitch-scale (100 kyr) cycles, and their subdivision into systems tract (forced regressive–FSST, lowstand–LST, transgressive–TST, highstand–HST) (from [Amorosi et al., 2014](#)). Note the basin-wide extent of the transgressive surface.

and from the eastern Apennine rivers is  $32.2 \times 10^6$  tons  $\text{yr}^{-1}$  and  $1.5 \times 10^6$  tons  $\text{yr}^{-1}$ , respectively North and South of the Gargano Promontory ([Cattaneo et al., 2003](#)). In spite of their smaller drainage areas, the cumulative sediment yield of the Apennine rivers doubles that of the Po River, mainly reflecting muddier catchment basins. Seasonal asynchronous flood cycles affecting distinctive reaches of the Po catchment result in bimodal river discharge and greatest concentrations of suspended load, with distinct peaks in spring and autumn, respectively ([Correggiari et al., 2005a; Syvitski et al., 2005](#)). A flux of  $568 \text{ kg s}^{-1}$  corresponds to an average concentration of suspended sediment of  $336 \text{ mg l}^{-1}$  at Pontelagoscuro (Fig. 1). The average monthly concentrations for April and December are about  $500 \text{ mg l}^{-1}$ , but under flood conditions monthly averages of 3100 to  $4350 \text{ mg l}^{-1}$  have been reported. Sediment flux is  $10.4 \times 10^6 \text{ m}^3 \text{ yr}^{-1}$  and sediment yield is  $214 \text{ tons km}^{-2} \text{ yr}^{-1}$  ([Syvitski et al., 2005](#)).

### 3. Middle-late Pleistocene record of Milankovitch-scale cyclicity

A ~100 kyr periodicity in sea-level change for the middle-late Pleistocene is well established ([Hays et al., 1976; Chappell and Shackleton, 1986](#)), and it is well known that 100 kyr, eccentricity-driven cycles reflect major changes in ice volume ([Lisiecki and Raymo, 2005](#)). The middle-late Pleistocene 100 kyr cycles are markedly asymmetric, with long phases of relative sea-level fall followed by short periods of stabilization and rise ([Waelbroeck et al., 2002](#)). This characteristic pattern records rapid phases of ice melting as opposed to comparatively longer periods of ice growth ([Lisiecki and Raymo, 2005](#)).

The ~100-kyr periodicity impacted significantly the stratigraphic architecture of Quaternary margins during the past ~800 kyr ([Lobo and Ridente, 2014](#)). In the Po Plain–Adriatic system, the Po Delta moved back and forth repeatedly during the middle-late Pleistocene, under the control of high-frequency sea-level fluctuations. The resulting poly-phased progradational history of the Po River generated a broad delta plain that was largely drowned during the modern high sea-

level interglacial, leading to the formation of the N-Adriatic shelf. This drowned shelf lies between the present Po Plain and the MAD, a 260 m-deep slope basin fed by river-borne fine-grained turbidites ([Trincardi et al., 1996; Ghielmi et al., 2013](#)). South of the MAD, a narrow shelf developed along the W-Adriatic margin, confined seaward by morphological highs that reflect deformation along the Apennine thrust-belt front. Most of the western shelf sector was starved during the glacial (lowstand) intervals because (i) it was progressively exposed during sea-level fall and lowstand phases ([Trincardi and Correggiari, 2000](#)); (ii) the Po River intercepted most of the Apennine rivers flowing from WNW and debouched as a “mega-river” into the MAD, depriving the area to the south of a greater part of the sediment discharge ([Ciabatti et al., 1987; Kettner and Syvitski, 2008](#)).

From a sequence-stratigraphic perspective, the ca. ~100-kyr middle-late Pleistocene cycles correspond to 4th-order depositional sequences. Each of them, in turn, is subdivided into its systems tracts components. In [Sections 5 to 8](#), we explore the stratigraphic architecture of the post-MIS5e interval across the Po Plain–Adriatic system, including the four systems tracts (forced regressive, lowstand, transgressive, and highstand) developed during the last cycle of relative sea-level fall and rise that followed the Last Interglacial (MIS5e).

#### 3.1. Onshore stratigraphy

The major architectural components of the Pliocene-Quaternary succession in the Po Basin stack to form a two-fold, cyclic hierarchy of (i) third-order depositional sequences (*sensu* [Mitchum et al., 1977](#)), about 100–1000 m thick, separated at the basin margin by tectonically formed angular unconformities (Fig. 2A); and (ii) fourth-order, transgressive-regressive sequences (Fig. 2B), approximately 50–100 m thick, controlled by glacio-eustatic fluctuations ([Amorosi et al., 2014](#)).

A cyclic vertical stacking of marine and continental deposits, with thicknesses of about 50–100 m, reveals the overprint on stratigraphic architecture of middle-late Pleistocene-Holocene sea-level and climate

fluctuations in the distal portion of the Po Basin (Fig. 2B). Above a regional unconformity dated to 0.87 Ma BP (Muttoni et al., 2003), eight transgressive-regressive (T-R) depositional cycles have been identified and physically tracked throughout the Po Basin (Ori, 1993; Regione Emilia-Romagna and Eni-Agip, 1998; Regione Lombardia and ENI-Divisione Agip, 2002; Amorosi et al., 2014 – Fig. 2B).

Distinctive cyclic changes in lithofacies and channel stacking patterns are the most prominent feature of the T-R sequences. On a basin scale, the transgressive surfaces are the most readily identifiable surfaces and represent the bounding surfaces of sedimentary packages that accumulated over time spans of ~100 kyr. These surfaces are basin-wide stratigraphic markers that demonstrate greater extent and correlation potential than the sequence boundaries or the maximum flooding surfaces (Bhattacharya, 2011). The T-R sequences are best recognized beneath the modern coastal plain and the delta, where typical transgressive-regressive coastal wedges form the transgressive and highstand systems tracts (TST + HST in Fig. 2B). The wedge-shaped shallow-marine bodies are separated by thick packages of alluvial deposits, representing the falling-stage and lowstand systems tracts – FSST + LST in Fig. 2B). In more internal positions, close to the basin margin, the T-R cycles consist of basal overbank facies with isolated fluvial-channel sand deposits. Upwards, a vertical transition to higher sand/mud ratios is observed, and the fluvial bodies become increasingly abundant, amalgamated and laterally continuous (LST), forming distinctive channel-belt sand bodies. Local variability in subsidence rates may cause variation in the vertical spacing of channel belts from site to site (see Wilson et al., 2014). Following Catuneanu et al. (2009), we use here the traditional sequence-stratigraphic nomenclature in lieu of the common partition of alluvial successions into low/high accommodation systems tracts (Olsen et al. 1995; Posamentier and Allen, 1999; Plint et al., 2001), because of the lateral correlation of fluvial architecture with shoreline transgressions and regressions.

### 3.2. Offshore stratigraphy

The middle-late-Pleistocene 100-kyr climatic and eustatic cyclicity observed in the Po Plain is also recorded offshore, and particularly in the outer-shelf region West and South of the MAD, where four eccentricity-driven cycles of sea-level change are recorded by as many regressive sequences (Piva et al., 2008a,b; Ridente et al., 2009). On the Central Adriatic Shelf these sequences are bounded by high-amplitude reflectors with very gentle seaward dips that truncate oblique-tangential clinoforms dipping seaward at angles typically fractions of a degree (Trincardi and Correggiari, 2000; Ridente and Trincardi, 2002). The four regressive sequences extend over distances of up to 300 km, from the Central to the South Adriatic Shelf and form a composite shelf wedge with contrasting stacking patterns, denoting distinct long-term margin behaviors with dominant tectonic subsidence in the Central Adriatic and increasing-landward uplift rates in the South. The depocenters of all sequences are elongated parallel to the basin margin and to the Tremiti high, which was emergent during each sea-level lowstand. In the Central Adriatic the four sequences form a composite backstepping shelf-perched wedge reflecting subsidence (Maselli et al., 2010). South of the Tremiti high, the depocenters of the four sequences are reduced in thickness and are more discontinuous, recording syn-sedimentary structural deformation of the margin in the vicinity of the Gargano Promontory (Ridente and Trincardi, 2002, 2006). Farther South, the four sequences show an overall seaward shift from the oldest to the youngest, defining a forestepping stacking pattern. Syn-depositional tectonic deformation is evident, particularly in the presence of inherited tectonic structures, the most evident of which is the Gondola deformation belt (Ridente and Trincardi, 2006).

In the context of PROMESS1, a European Union project, two continuous-recovery boreholes (PRAD1-2 and PRAD2-4) were drilled in the Central Adriatic, in 186 m water depth on the upper slope, and in 54 m on the inner shelf, respectively (Fig. 3). Borehole PRAD1-2

penetrated 71.2 m through a stratigraphic interval characterized by sub-parallel seismic reflections and uniform seismic units. Based on an age-depth model grounded on several independent proxies (including foraminifer and nannoplankton stratigraphy,  $d^{18}\text{O}$  curves, magnetostratigraphy, tephra stratigraphy and, for the upper part,  $^{14}\text{C}$  dating) the cored interval records Marine Isotope Stages (MIS) from MIS1 to the top of MIS11, thus encompassing the past 370 kyr (Piva et al., 2008a,b; Bourne et al., 2010). This continuous record through the last four glacial-interglacial cycles from a proximal continental slope setting indicates that margin progradation occurred dominantly during interglacial intervals (MIS5, MIS7, and MIS9), and appears composed of thicker packages formed during the interstadials, with thinner forced-regressive systems tracts (FSST) deposited during stadial periods above distinctive downward shift surfaces (Ridente et al., 2009). The development of interstadial deposits with distinctively thicker and more extensive bottomsets reflects enhanced shore-parallel advection any time sea-level rise led to the drowning of the Adriatic shelf, likely triggering the formation of dense water and vigorous cyclonic circulation. This advection mechanism persisted in each cycle, progressively decreasing as sea-level fall approached the maximum lowstand position, when most of the shelf became exposed.

## 4. Data and methods

This review paper relies on data partially published in previous papers focused on specific aspects of the evolution for individual components of the Po Plain–Adriatic system. On land, stratigraphic correlations have been built upon a high-quality data base with extensive core control, and refined facies analysis represents the building block for sequence stratigraphic analysis. Over 250 continuous cores (Fig. 4), 30–175 m long, recovered by the Emilia-Romagna Geological Survey during the 1990s and the 2000s as part of the Geological Mapping Project of Italy to 1:50,000 scale, were analyzed in detail over the last 20 years. Facies characterization was carried out through multi-proxy investigations on a significant part of these cores, including mollusks (Scarpioni and Kowalewski, 2004, 2007; Scarpioni et al., 2013; Wittmer et al., 2014; Kowalewski et al., 2015), the meiofauna (Amorosi et al., 1999a,b, 2003, 2005, 2008a; Rossi and Vaiani, 2008; Rossi and Horton, 2009; Dinelli et al., 2013), pollen (Amorosi et al., 1999b, 2004, 2008b), sand petrography (Marchesini et al., 2000), and whole-rock geochemistry (Amorosi et al., 2002, 2007; Bianchini et al., 2002, 2012; Curzi et al., 2006; Amorosi and Sammartino, 2007, 2014; Amorosi, 2012). Facies calibration and mapping have been complemented by data from thousands of core descriptions and piezocene penetration tests made available by the Emilia-Romagna Geological Survey. All facies and sediment provenance information reported in this paper summarizes this large body of research.

Offshore, the database collected by ISMAR over the last 20 years includes more than 800 gravity and piston cores (typically <15 m in recovery), 2 long cores (boreholes PRAD1-2 and PRAD2-4) collected within the EU project PROMESS-1, and a total of 80,000 km of high-resolution seismic profiles using a 16-transducers hull-mounted CHIRP-sonar source (Fig. 4). In addition, the data set includes single-trace 1-kJ sparker profiles and a small set of high-resolution multi-channel profiles collected firing a S30 Water gun source, and recorded with a 48-channel streamer with typical trace interval of 6.25 m.

Stratigraphic correlations across the shoreline in a source-to-sink frame are not straightforward. Acquisition, investigation and interpretation of stratigraphic and sedimentological data in the subaerial and submarine realms bear intrinsic differences: on land, drilling operations, including continuously-cored boreholes and piezocene penetration tests are relatively inexpensive compared to prices offshore, and a dense network of 30–40 m long boreholes may provide a sound basis for physical correlation of the key surfaces and facies characterization of late Quaternary deposits. On the other hand, high-resolution geophysical data are difficult to acquire, for both technical and logistical

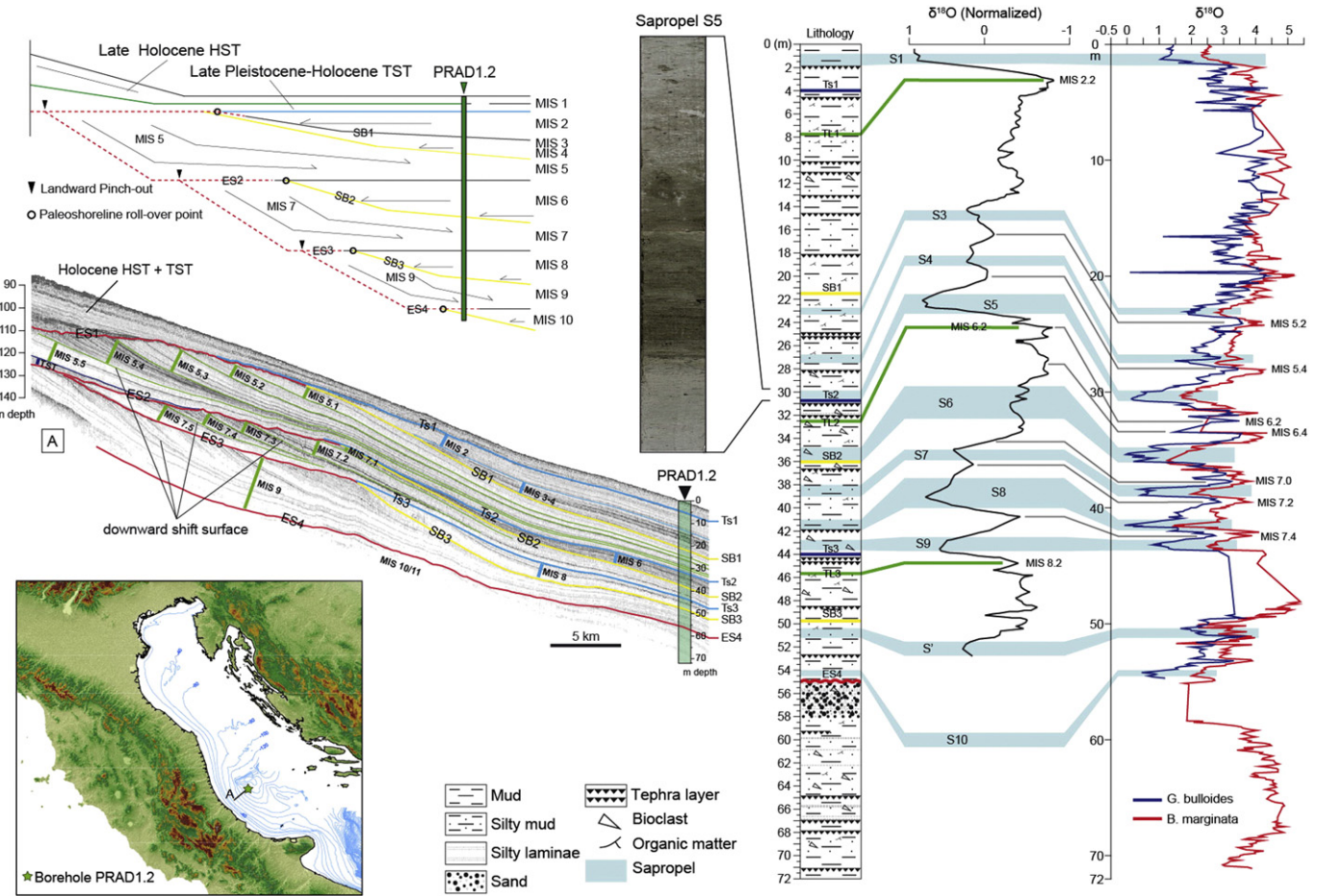


**Fig. 3.** Synthetic view of the stratigraphy of PRAD1-2 (right column) in the Central Adriatic (location map is bottom left), with high-resolution CHIRP sonar profile (central, left) and stratigraphic scheme (upper, left). The stratigraphy of PRAD1-2 relies on a multi-proxy set of analyses including tephra determination (Bourne et al., 2010) and oxygen stable-isotope curves (planktic foraminifer *Globigerina bulloides* and benthic foraminifer *Bulimina marginata* are reported in blue and red, respectively) accompanied by the recognition of "Sapropel-Equivalent" beds (S1 to S10; Piva et al., 2008a,b). Sapropel S5 is documented on photograph as a laminated dark interval with higher content of organic matter (never reaching the 2% or higher TOC values typical of the deep environments of the Eastern Mediterranean, but sharing the same micropaleontological assemblage). The seismic profile shows that margin progradation occurred mostly during interstadial intervals, when the shelf was flooded, and decreased when the shelf was exposed (Ridente et al., 2008, 2009; Maselli et al., 2010).

reasons. Specifically, the upper few tens of meters below the ground typically provide inconsistent or poorly resolved reflection geometries. Furthermore, alluvial and coastal plains are densely populated areas, and permits for geophysical surveys can be very hard to obtain.

In marine environments, seismic-stratigraphic data can be collected in nested multi-frequency surveys with complementary spatial and vertical resolution, and key reflections in undeformed settings can be traced over hundreds of kilometers. Coring is commonly achieved only for the upper 10 m below the seafloor, while longer boreholes require extremely expensive research projects (PROMESS1, in the Adriatic is an example). In addition, oil companies in their search for suitable reservoirs in the deep subsurface normally wash their boreholes in the upper several tens to few hundred meters below sea floor, thereby losing the opportunity to collect data from the late Quaternary sedimentary packages. The coastal zone also presents difficulties for the acquisition of geophysical offshore data: reverberation increases dramatically as the seafloor shoals, and shallowly buried biogenic gas may further hamper signal penetration.

## 5. Forced regressive systems tract (~115–30 cal kyr BP)

### 5.1. Onshore stratigraphy

The Po Plain is a high-accommodation setting characterized by huge stratigraphic expansion. Contrary to the early sequence-stratigraphic

models (Posamentier et al., 1988; Posamentier and Vail, 1988), which postulate a typical mechanism of incision and complete sediment bypass in response to relative sea-level fall at the basin margin, the Po Plain preserves an unusually thick record of forced-regressive (or falling stage – Plint and Nummedal, 2000) deposits (see discussion in Blum and Törnqvist, 2000; Blum et al., 2013). Tectonic subsidence in this area was locally able to compensate for subsequent middle to late Pleistocene relative sea-level fall, allowing accommodation creation and accumulation of alluvial plain deposits even during intervals of forced regression. As a consequence, the thickness of the MIS5e–MIS2 succession in the subsurface of the Po Plain may exceed 100 m (Amorosi et al., 2004).

Two prominent stratigraphic markers, corresponding to wedge-shaped coastal sand bodies with very similar internal architecture, are recurrently recorded beneath the modern coastal plain, at 0–30 m and 100–120 m core depth intervals, respectively (Amorosi et al., 2004 – Fig. 2B). These nearshore to shallow-marine packages, corresponding to transgressive and highstand deposits (see Sections 7.1 and 8.1), can readily be tracked in the subsurface of the Po Plain, parallel to the Adriatic shoreline, and bracket a thick succession of mud-prone, extensively pedogenized alluvial deposits (FSST and LST in Fig. 2B). Following the south-sloping Pedealpine homocline, the MIS5e coastal sand body is identified at progressively lower depths north of the Po Delta, into the subsurface of the Venetian and Friulian coastal plains (Ferranti et al., 2006), thus confirming the crucial role played by tectonic subsidence in shaping the Po Basin fill (see also Carminati et al., 2003).

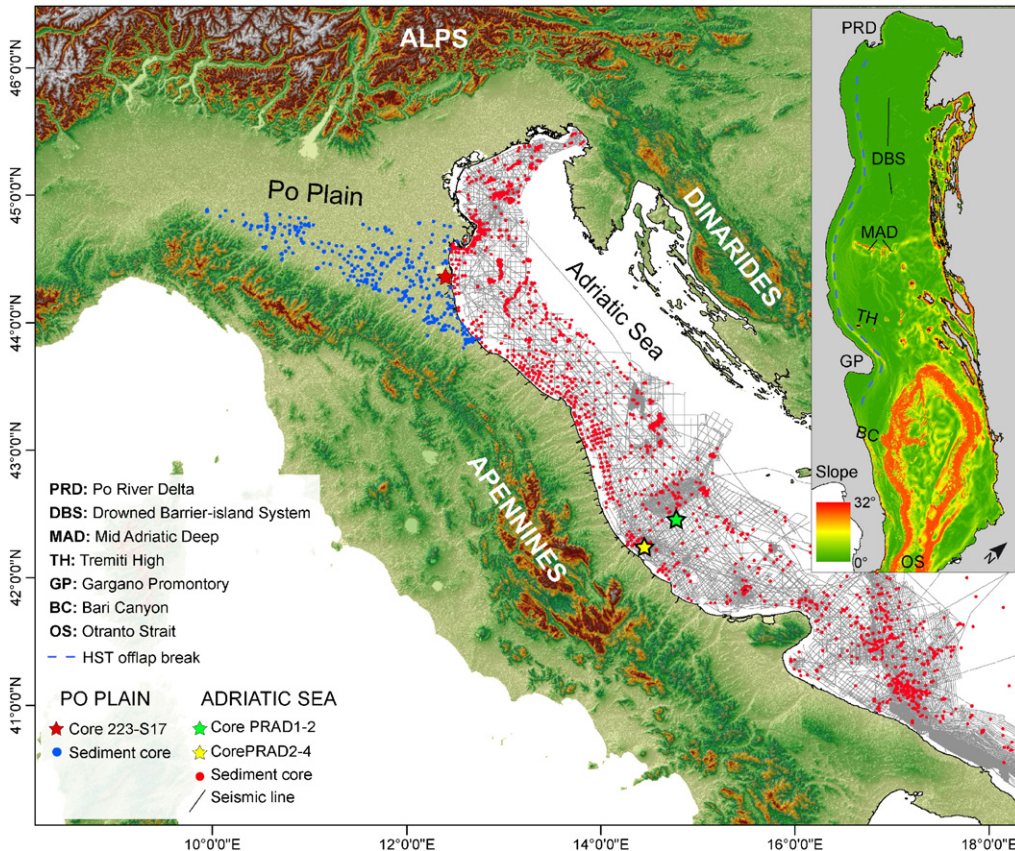


**Fig. 4.** Geophysical and sediment core data set used to study the whole Po Plain–Adriatic system. For the onshore part, only 250 continuously cored boreholes are reported. Inset: sea floor slope map of the Adriatic Basin.

A nearly continuous record of post-MIS5e stratigraphy in the Po Plain has been documented by two long-cored pollen profiles (Amorosi et al., 2004, 2008b) and by their correlation with coeval pollen series from southern Europe (Woillard, 1978; Follieri et al., 1988; Tzedakis et al., 1997). Pollen spectra from Core 223-S17 provide independent chronologic constraints, and highlight the combined effect of sea-level and climate changes on cyclic facies architecture (Fig. 5). The onset of transgressive, nearshore sedimentation in the Po Plain was invariably accompanied by repeated expansions of oak (*Quercus*) forests, a pollen signature diagnostic of warm climate (interglacial) periods. In contrast, transition to stable continental environments during phases of relative sea-level fall is fingerprinted by very low pollen concentrations, showing the development of shrubby-herbaceous communities, with parallel expansion of *Pinus* and the retreat of the temperate woodlands. These pollen types reflect the onset of a cold climate vegetation characteristic of stadial to fully glacial conditions.

Weaker expansions of broad-leaved and/or coniferous (excluding *Pinus*) arboreal vegetation (see the AP1 + AP2 profile in Fig. 5) indicate episodes of climatic amelioration that have been interpreted as interstadials. Three episodes of relative climate warming, marking the MIS5c, MIS5a, and MIS3 interstadials, respectively, are invariably related to minor transgressive pulses, documented by the development of laterally extensive paludal/lagoonal horizons within the monotonous continental succession (Amorosi et al., 2004). A primary control of glacio-eustatic fluctuations on facies architecture is confirmed by the striking coincidence between the AP1 + AP2 profile and the relative sea-level curve for the last 150 kyr (Fig. 5).

Upstream persistence of vegetation contrasts between glacial and interglacial facies successions is robust in the Po Basin and suggests that depositional processes and alluvial facies were strongly coupled to the prevailing climate conditions (Blum and Aslan, 2006). Landwards of the line of maximum shoreline migration, the diagnostic record of

glacial/interglacial transitions, i.e. thermophilous forest expansions, is observed at the base of thick intervals of overbank fines on top of laterally extensive fluvial channel belts (Amorosi et al., 2008b – Fig. 2B). This pollen signal documents that the major phases of channel abandonment and widespread floodplain aggradational in the central Po Plain took place at the onset of warm-temperate (interglacial) climatic conditions, in association with (or, possibly, in response to) phases of rapid sea-level rise.

## 5.2. Offshore stratigraphy

The youngest Pleistocene sequence records the interval from the MIS5e sea-level highstand to the onset of the LGM (Fig. 6); subtle variations in the internal seismic-reflection patterns reflect the stacking of distinct systems tracts (Ridente and Trincardi, 2002, 2005). Packages of landward onlapping, plane-parallel reflectors are locally found within the basal portion of the depositional sequence; in particular, the basal seismic unit characterized by landward-onlapping plane-parallel reflections is interpreted as a transgressive deposit (TST). The overlying multiple stack of progradational clinoforms is interpreted as a succession of highstand to forced-regressive wedges deposited as a continuum with gradually seaward increasing clinoform angles. Highstand deposits (HST) can be tentatively distinguished from forced-regressive deposits (FSST), because internal seismic reflectors in the HST are structured as very low-angle oblique-tangential clinoforms with well-developed plane-parallel bottomset drapes; the FSST includes progressively steeper oblique-tangential clinoforms, with sharper downlap and reduced distal drape, where present (Ridente and Trincardi, 2002).

The uppermost FSST has a distinctive internal architecture and lithologic composition compared to the underlying forced-regressive deposits of the same sequence. This unit (Distal Forced-Regressive Wedge or DFRW) is characterized by a concave, high-amplitude basal

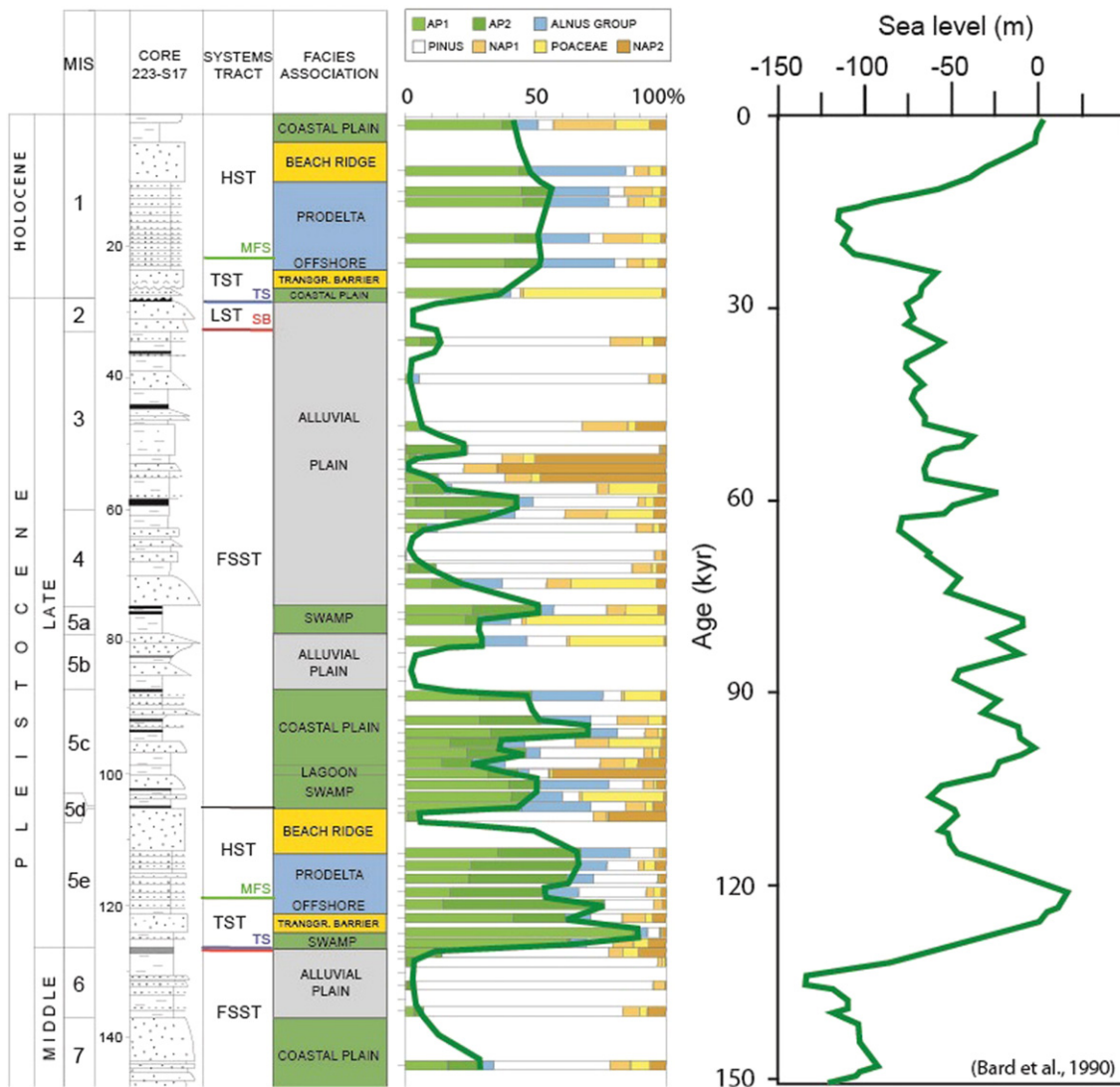


**Fig. 5.** Pollen profile from Core 223-S17 (see Fig. 4, for location), showing vegetation changes during the last 150 kyr (MIS 6 to MIS 1) and sequence-stratigraphic interpretation. Note the striking similarity between the arboreal pollen (AP1 + AP2) profile and the sea-level curve (from Bard et al., 1990). AP1: mesophilous elements (deciduous broad-leaved trees, with *Quercus* as the main component); AP2: altitudinal trees (*Fagus*, *Abies*, and *Picea*); ALNUS GROUP: riparian trees; *Alnus*, *Salix* and *Populus*; NAP1: non-arboreal elements, excluding NAP2 and *Poaceae*; NAP2: shrubs and herbs withstanding dry conditions (*Artemisia*, *Ephedra*, cf. *Cupressaceae*, *Armeria*, *Chenopodiaceae*, *Hippophae*). FSST: forced-regressive systems tract, LST: lowstand systems tract, TST: transgressive systems tract, HST: highstand systems tract, SB: sequence boundary, TS: transgressive surface, MFS: maximum flooding surface.

reflection, a convex top reflection and a markedly irregular internal seismic-reflection pattern, with closely-spaced diffraction hyperbolae, that has no equivalent in the older forced-regression units (Ridente and Trincardi, 2005). The basal reflection of the DFRW is a marked downlap surface, interpreted to represent the last steps of sea-level fall that led to the last glacial lowstand. The top reflection of the DFRW merges landward with the shelf-wide unconformity and becomes conformable seaward. Cores that penetrated DFRW North and South of the Gargano Promontory show cm-scale layers of fine sand, indicating a coarsening-upwards trend relative to the older forced-regressive units (Ridente and Trincardi, 2005).

## 6. Lowstand systems tract (~30–18 cal kyr BP)

### 6.1. Onshore stratigraphy

Several sequence-stratigraphic models have predicted the presumed position of paleosols within non-marine deposits (Van Wagoner et al., 1990; Wright and Marriott, 1993; Hanneman and

Wideman, 2006; Cleveland et al., 2007; Mack et al., 2010; Gibling et al., 2011; Varela et al., 2012), and the role of paleosols formed at interfluvial sequence boundaries (i.e. adjacent to paleovalley systems, during prolonged periods of channel entrenchment) has also been highlighted by sequence stratigraphy (Van Wagoner et al., 1990; Gibling and Bird, 1994; Gibling and Wightman, 1994; Aitken and Flint, 1996; McCarthy and Plint, 1998; Plint et al., 2001). These models, however, mostly rely upon combinations of well log, outcrop and seismic data from the ancient record, where chronologic control of alluvial sedimentation is extremely limited. In this regard, the Po Plain may serve as an intriguing Quaternary analog with high-resolution chronology.

In the subsurface of the Po Plain, closely-spaced paleosols of latest Pleistocene age form prominent stratigraphic markers across lithologically homogeneous overbank fines, and are laterally associated with channel-belt development (Fig. 7A). Particularly, the repeated alternation of pedogenized horizons with non-pedogenized alluvial strata, forms aggradationally stacked, paleosol-bounded packages, a few m thick, that can be physically tracked over distances of tens of km (Amorosi et al., 2015). These paleosols are weakly developed, with

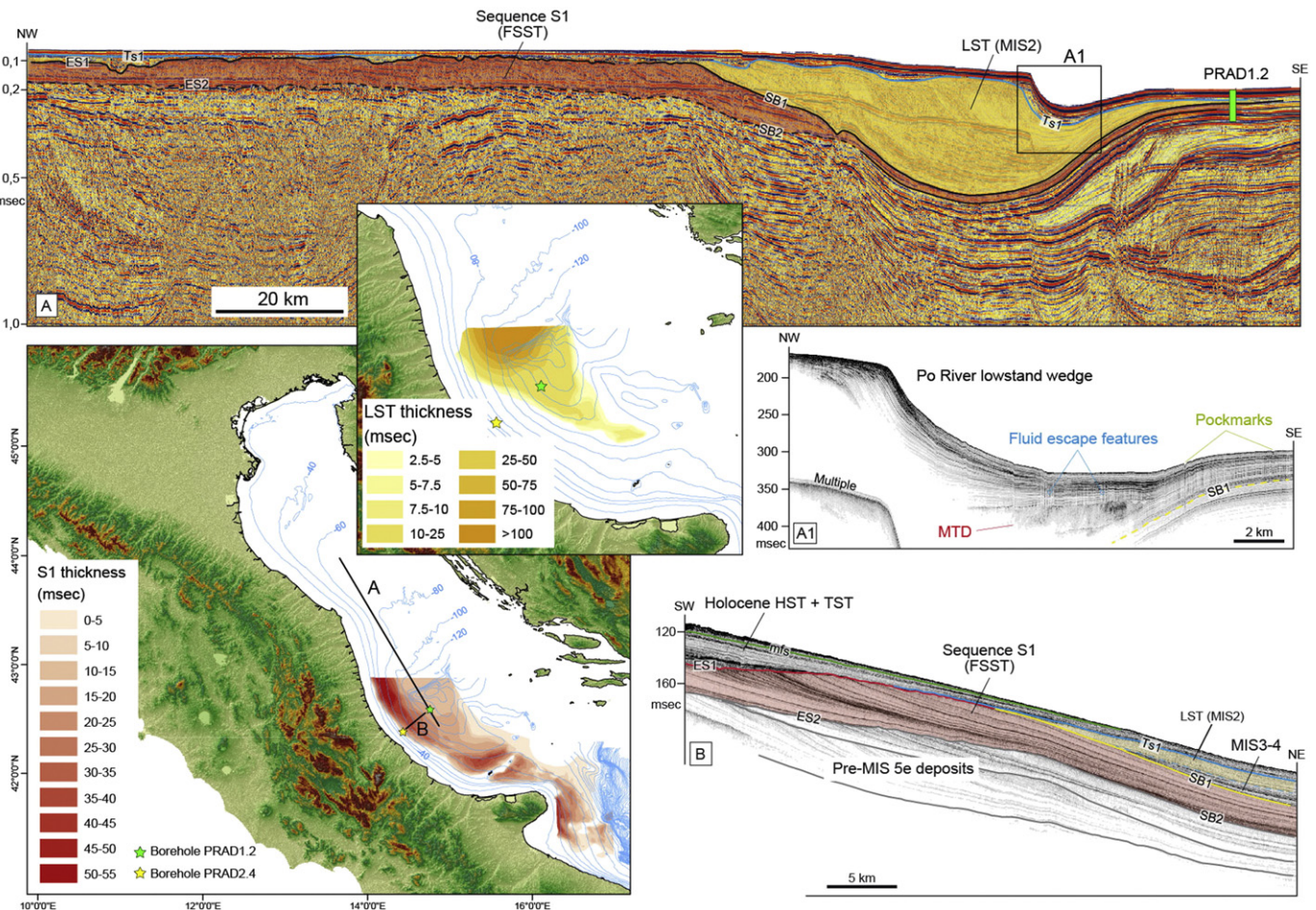


**Fig. 6.** Multichannel seismic profile RF95-1/2 (modified from Trincardi et al., 1996; Maselli et al., 2011) showing the thick (350 m) Po River lowstand delta (LST) during the Last Glacial Maximum (LGM) and its correlative unconformity through the alluvial/coastal plain domain to the north (left). The thickness map of the LST delta is shown in the central inset. A1: high-resolution CHIRP sonar profile showing a detail of the alluvial plain deposits at lowstand. Surface ES1 represents a reworked correlative of the sequence boundary (SB1; Ridente and Trincardi, 2002). The MCS profile also shows the occurrence of a thick wedge of FSST deposits below the sequence boundary; a higher-resolution profile from the western flank of the MAD (bottom right) shows in detail the internal geometry of muddy FSST deposits encompassing the interval between MIS5 and MIS3. The thickness distribution of this unit is reported in the map inset at the bottom left.

A-Bw-Bk-C profiles (Inceptisols of Soil Survey Staff, 1999 – Fig. 8A), and mark short-lived phases of subaerial exposure, in the range of a few thousand years.

Paleosols can be identified on the basis of a variety of subsurface proxy data, including facies analysis on cores, paleopedological data, geotechnical properties and piezocene penetration tests (Amorosi et al., 2014). The high potential of the engineering properties of sediments for the high-resolution stratigraphy of unconsolidated Quaternary deposits has been illustrated by Amorosi and Marchi (1999), who demonstrated that paleosol identification can be carried out through the combination of cone tip penetration, sleeve friction and pore pressure values. Pocket penetrometer resistance, a supplementary information normally available from most core descriptions, may serve as a reliable, additional tool for paleosol recognition and stratigraphic profiling (see facies characterization in Table 1 – Amorosi et al., 2015).

Based on radiocarbon dates (Fig. 7A), soil development appears to be coeval with the long phase of sea-level fall and climate cooling that occurred after the MIS5–MIS4 transition, especially at the transition between MIS3 and MIS2 (FSST/LST boundary). Fluvial incision into older alluvial deposits likely took place under a mixed, climatic and eustatic control (Amorosi et al., 2014). The well-developed paleosol formed at the onset of the Last Glacial Maximum (red line in Fig. 7) is interpreted to represent the sequence boundary. This

horizon is laterally traceable off the interfluvia into a highly diachronous surface at the base of laterally extensive fluvial-channel bodies (Figs. 7 and 8B).

Despite objective difficulties in defining the style and character of the fluvial systems from relatively sparse subsurface data, it is apparent that lowstand deposition was characterized by well-defined channel-belt sand bodies, with a relative abundance of channel facies and paucity of floodplain deposits (Fig. 7). Fluvial stratigraphic architecture varies along an axis-to-margin transect. A higher proportion of channel belts and splays is observed in the axial part of the system, where the Po River exhibits larger and thicker channel belt sand bodies, with higher net-to-gross than their Apennine counterparts (Amorosi et al., 2014).

The Po channel-belt sand body commonly exceeds 20 km in width (Fig. 7A). Laterally amalgamated fluvial bodies are interpreted as deposits of braided- and low-sinuosity rivers that developed under conditions of increased sediment supply. Low accommodation during lowstand phases possibly favored lateral migration of river channels, with widespread development of scour-and-flood episodes. The multi-storey character of the channel belts, which may exceed 30 m in composite thickness, suggests continuous creation of accommodation by tectonic subsidence, which resulted in the storey architecture, with high degree of amalgamation and channel connectivity (Fig. 7A).

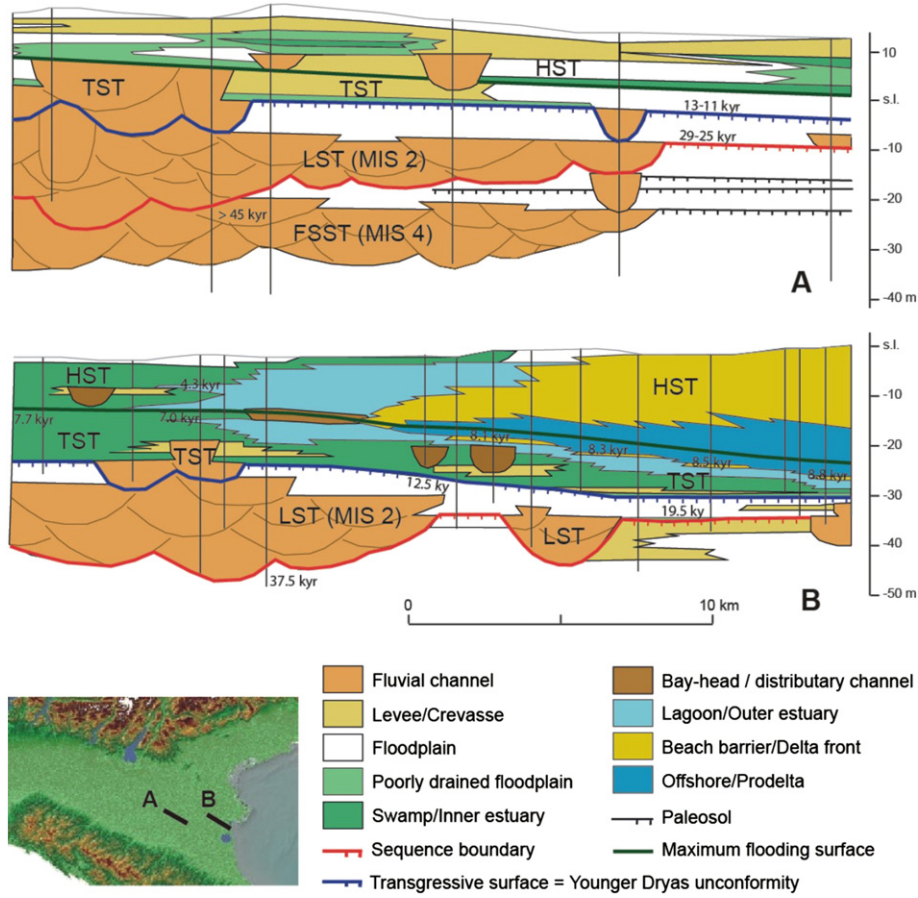


**Fig. 7.** Systems tract architecture of the late Pleistocene-Holocene succession at the southern margin of the Po channel belt. A. Stratigraphic relation between paleosols and amalgamated fluvial lowstand (LST) and forced-regressive (FSST) sand bodies. B. Characteristic transgressive-regressive architecture of transgressive (TST) and highstand (HST) deposits atop the lowstand channel belt. Note the backstepping and forestepping pattern of millennial- to centennial-scale parasequences, highlighted by shoreface deposits and their age. Approximate radiocarbon dates from Amorosi et al. (2003), Scarpioni et al. (2013) and the Emilia-Romagna Geological Survey database. The transgressive surface largely coincides with the prominent (Younger Dryas) paleosol at the Pleistocene-Holocene boundary, with local re-incision of the lowstand channel belt. Ages are reported as cal kyr BP.

## 6.2. Offshore stratigraphy

The Adriatic basin presents an exceptionally thick LST formed during the LGM and partitioned in two main depositional domains: an extensive alluvial plain, corresponding to the modern, low-gradient Adriatic shelf (North of the MAD; Fig. 6), and a shelf-edge delta, over 350 m thick, which constitutes the northern flank of the MAD (Trincardi et al., 1996; Maselli et al., 2011). The alluvial-plain depositional system is difficult to resolve entirely on high-resolution seismic profiles, because of the high reverberation and limited signal penetration across over-consolidated clays and/or because it is deeply buried below younger TST and HST deposits along a mud belt that parallels the Italian coast. Away from this mud belt, the alluvial plain deposits show, in sediment cores, terrestrial gastropod faunas and peat horizons, locally accompanied by sandier crevasse splay units. The alluvial depositional system is characterized by aggradational packages, a few tens of meters thick, and by a complex set of shallowly cut channelized features. Despite the dense grid of geophysical data, no major valley systems have been observed. The thick lowstand delta North of the MAD is dominantly composed of muddy units deposited rapidly during the LGM, and likely recording short-term sediment supply fluctuations and lobe switches (Trincardi et al., 1996). The deltaic deposits are organized in sigmoidal clinoform, with an overall weakly aggradational shoreline trajectory, where the sand component is restricted to the topset region and the bulk of the clinoform is fine-grained. Distally, the clinoform pass into a basin-floor section consisting of thin-bedded

turbidity-current deposits that pinch out toward the southern flank of the MAD (Fig. 9).

The lowstand systems tract includes an extensive acoustically transparent deposit ponded in the topographic low of the MAD underneath the LGM lowstand delta (Fig. 6). This deposit displays an irregular upper surface and a chaotic or transparent internal seismic facies, indicating a lack of coherent stratification, likely in response to mechanical remolding. Despite its thickness, this deposit does not prevent penetration of the high-frequency acoustic signal from CHIRP sonar below its base and, in the lack of direct sampling, can be considered likely dominantly muddy (Trincardi et al., 2004; Fig. 6). Stratigraphic position of the mass-transport deposit is within the lower portion of the lowstand wedge. Therefore, it is not equivalent to that of a basin-floor fan, sensu Hunt and Tucker (1992), located immediately above a sequence boundary and beneath a lowstand wedge. Similar mass-transport deposits formed within lowstand wedges at the expense of selected clinoform wedges during previous Pleistocene sea level cycles (Dalla Valle et al., 2013b), suggesting that accumulation rate is a main predisposing factor for this type of sediment failure.

The sequence boundary marks the top of the forced-regressive wedge prograding from the South and West toward the MAD (Ridente and Trincardi, 2002). Dating of the deposits below the pinch-out of the acoustically transparent deposit (Trincardi et al., 1996; Piva et al., 2008a,b) and above the progradational wedge (Asioli et al., 1999, 2001), indicates an age of between 30 and 18 cal kyr for the Po lowstand

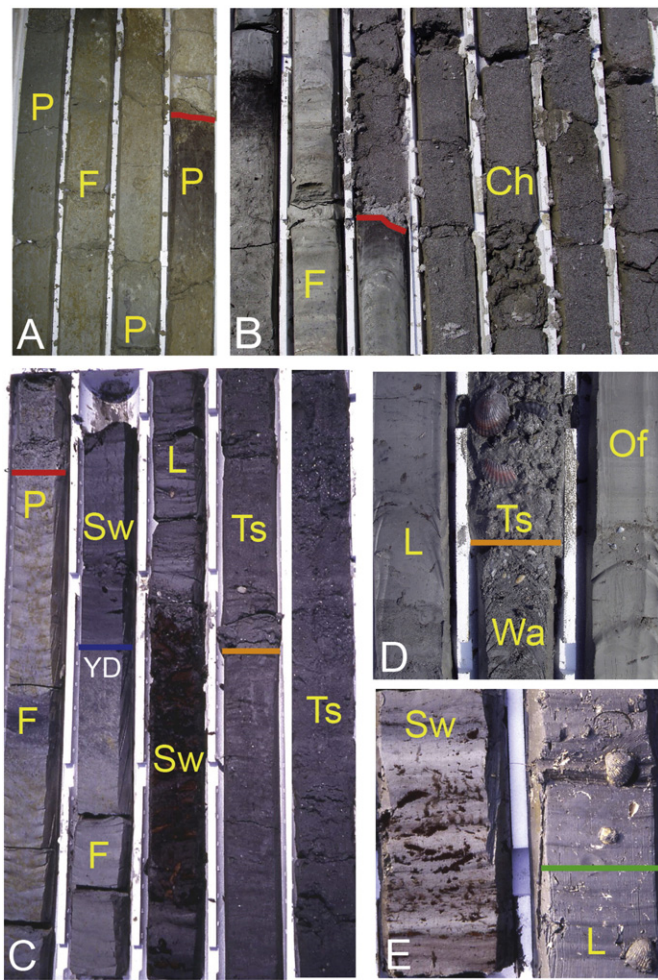


**Fig. 8.** Representative core photographs from the subsurface of the Po Plain, depicting vertical stacking of lowstand (LST) and transgressive (TST) facies associations, with related key surfaces for sequence stratigraphic interpretation. A: pedogenized floodplain (F) succession, with closely-spaced paleosols (P) capped by a composite, interfluvial sequence boundary (red line). B: sequence boundary (red line) separating the lowstand Po channel belt (Ch) from older floodplain deposits (F). C: characteristic deepening-upward succession of swamp (Sw), lagoonal (L) and transgressive shoreface (Ts) facies (TST) onto lowstand and older floodplain deposits (F). The red line is the sequence boundary (P = paleosol), the blue line is the transgressive surface (YD = Younger Dryas paleosol), the orange line is the ravinement surface (orange line) separating back-barrier (lagoonal – L and washover – Wa) facies from shallow-marine (transgressive shoreface – Ts to offshore – of) deposits (TST). E: maximum flooding surface (green line) landwards of the line of maximum shoreline migration, within lagoonal (L) deposits onto transgressive swamp (Sw) facies. Core bottom is lower left corner. Core width is 10 cm.

delta, above the mass-transport deposit (transparent unit), thus encompassing the LGM.

## 7. Transgressive systems tract (18–6 cal kyr BP)

### 7.1. Onshore stratigraphy

Beneath the modern coastal plain and the Po Delta, the transgressive surface (maximum regressive surface of Catuneanu et al., 2009) separates lowstand glacial deposits from an overlying, typically deepening-upward succession, formed under interglacial conditions (Figs. 7B and 8C). Initial flooding on the interfluves is generally marked by the sharp lower boundary of Holocene organic-rich swamp or poorly-drained floodplain deposits (Fig. 7). These facies associations commonly overlie pedogenized, well-drained Late Pleistocene floodplain deposits (Figs. 7 and 8C). The transgressive surface is easily recognizable on the

**Table 1**

Facies association	Thickness	Lower boundary	Lithology	Grain-size trends	Fossils	Common pocket penetration values (kg/cm <sup>2</sup> )	Sedimentary structures and accessory components
Fluvial channel	2–30 m	Erosional	Gravel to fine sand	FU	Rate (reworked)		
Levee Crevasse	0.5–2 m 0.5–2 m	Gradational Erosional (channel) gradational (spay)	Fine sand–silt alternation Medium to fine sand	FU (channel) CU (spay)	Barren Barren		Basal pebble lag, rip-up clasts, high-angle cross-lamination, amalgamation surfaces
Floodplain	1–30 m	Sharp/gradational	Silt and clay	FU (channel)	Barren	1.2–2.5 (paleosol 3–5)	Root traces, ripple-drift cross-lamination Flat lamination, high-angle cross-lamination
Poorly drained floodplain	1–5 m	Sharp/gradational	Silt and clay, locally organic-rich	FU (channel)	Rare freshwater	0.8–1.2	Root traces, mottling, brownish color, yellow to red hues common, Fe and Mg oxides, abundant paleosols
Distributary channel/bay head delta	1–6 m	Erosional (channel) gradational (delta)	Medium to fine sand	FU (channel) CU (delta)	Rare (transported)		Grey colour dominant, wood fragments, rare paleosols
Swamp/inner estuary	1–15 m	Sharp/gradational	Organic-rich clay and peat	CU	Common freshwater	0–1.2	Dark grey to black color, wood fragments
Lagoon/bay/outer estuary	1–10 m	Sharp/gradational	Clay (proximal) to sand-clay alternation (distal)	FU	Brackish (mud), transported marine assemblage (sand) Mixed nearshore assemblage	0.2–1.2	Wood fragments (proximal), mollusc shells (distal)
Transgressive barrier	0.5–2 m	Erosional	Medium to very fine sand	FU	Open marine, high diversity, transported (sand)	0.2–0.8	Basal fossiliferous lag
Offshore transition/offshore	1–3 m	Gradational	Sand–silt to silt–clay alternation	FU	Open marine, low-diversity, fluvial influenced	0.2–0.8	Bioturbation, storm layers, waning ripples
Prodelta	3–20 m	Gradational	Clay	CU	Nearshore (transported)		Wood fragments, flood layers, <i>Turritella</i> layers
Delta front/strandplain	6–12 m	Gradational	Coarse to very fine sand	CU			Abundant cross-stratification, bioclastic debris

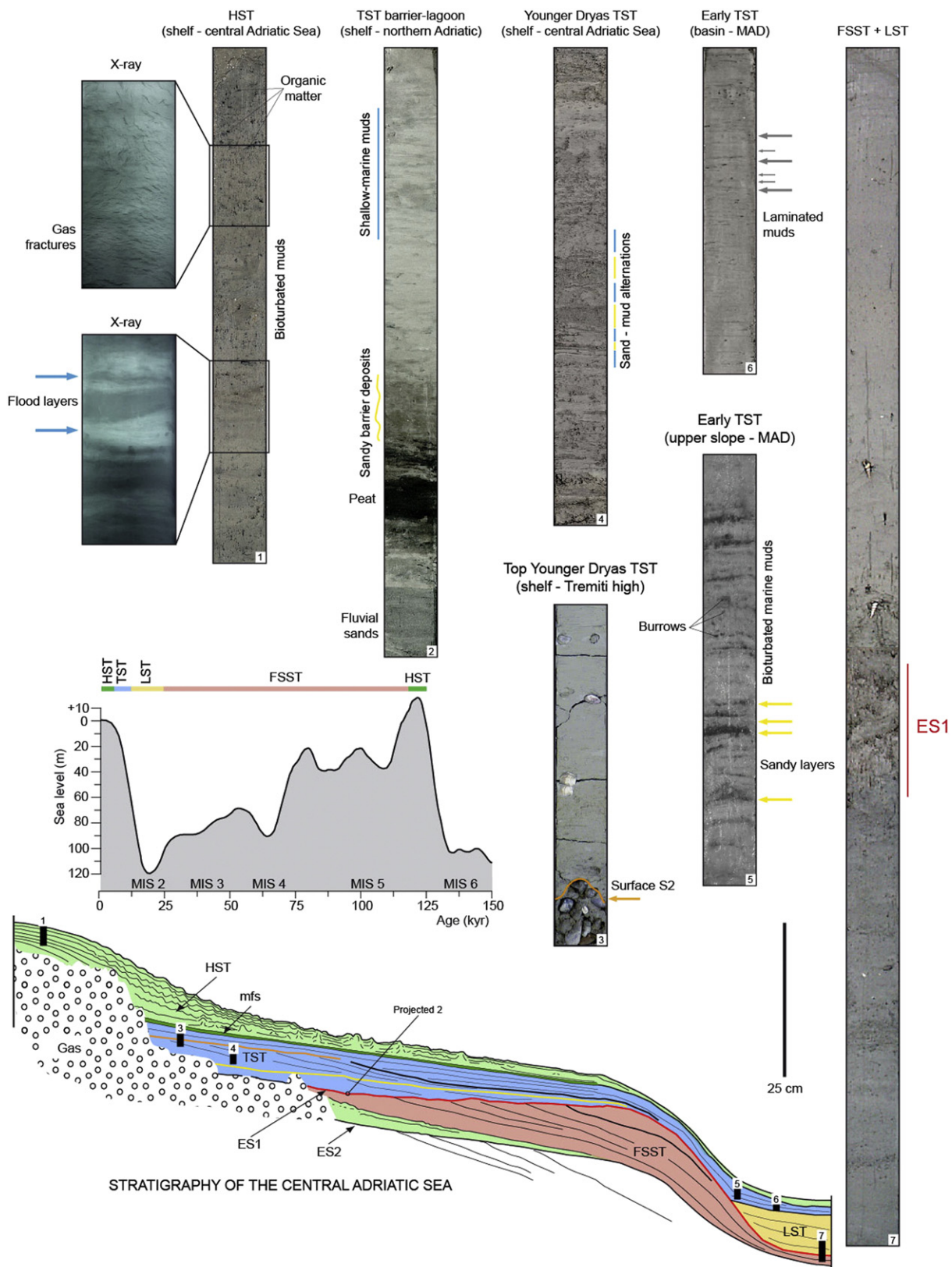


**Fig. 9.** Representative sediment core photographs from the offshore domain of the Adriatic Sea ideally positioned on a margin-normal geologic section: from left to right cores come from increasingly deep water and older sedimentary sections. HST deposits are dominantly muddy, locally gas-charged, typically intensely bioturbated, but may contain beds recording flood events (upper left); TST deposits (central cores 2 to 5) range from fluvial sand, peat deposits from back-barrier lagoons, to offshore muds, either homogenous or containing sharp-based sand beds recording river floods; locally, erosional surfaces within the TST are associated with pebble lags (Surface S2 in core 3, offshore Tremiti Islands). Core 7, on the right, shows the transition between FSST and LST deposits across surface ES1 on the flank of the MAD.

basis of its lithologic properties, and has a high correlation potential. At these locations, the transgressive surface and the sequence boundary are commonly separated by a few meters of floodplain deposits (Figs. 7 and 8C). The vertical transition from fluvial-dominated facies to overlying swamp and then lagoonal deposits indicates replacement of fluvial systems by estuarine environments in response to relative sea-level rise (Amorosi et al., 2003). Landwards, where the late Quaternary succession is made up entirely of non-marine deposits, as predicted by classic sequence-stratigraphic models (Wright and Marriott, 1993; Shanley and McCabe, 1994) the updip expression of the transgressive surface recognized at distal locations is a prominent, widespread surface marking the abrupt change in fluvial architecture, from laterally amalgamated (below) to isolated (above), ribbon-shaped fluvial bodies (Fig. 2B).

The transgressive surface also has a diagnostic pollen signature (Amorosi et al., 2004), marking the abrupt transition from glacial to interglacial pollen assemblages (Fig. 5). As a consequence, vegetation changes documenting the turnaround from glacial to interglacial conditions may be regarded as an efficient, separate tool to approximate the transgressive surface in areas far from marine influence (Amorosi et al., 2008b). This approach is especially useful within fully continental successions, where unequivocal indicators of relative deepening are lacking.

A weakly developed paleosol (inceptisol), with characteristic A/Bw/Bk profile, represents an additional stratigraphic marker of regional importance for the LST/TST boundary (YD in Figs. 7 and 8C). This paleosol can be tracked on land up to the Apennine foothills (Amorosi et al., 2014) and encompasses the Pleistocene-Holocene boundary. Based upon radiocarbon and pollen data, this paleosol has been related to the Younger Dryas (YD) cold reversal, a short-lived cooling event that preceded the onset of the Holocene, and the ultimate establishment of warm temperate climate conditions (Amorosi et al., 2003, 2014). The hiatus recorded by the YD paleosol is of about 2000–3000 years, and represents the time over which this surface was exposed before renewed transgression took place. This paleosol has distinctive geotechnical signature (Amorosi and Marchi, 1999) and can be tracked north of the Po Plain into the Venetian-Friulian plain and in the subsurface of Venice (see 'Caranto' paleosol in Fontana et al., 2008; Donnici et al., 2011). The YD paleosol is related to a short-lived phase of fluvial incision that locally re-incised the lowstand channel belts, resulting in vertically amalgamated sediment bodies (TST fluvial-channel bodies in Fig. 7).

Above the YD paleosol, the TST is characterized by a complex mosaic of coastal facies with distinctive backstepping architecture (Fig. 7B) that reflects the Holocene landward migration of barrier-lagoon and wave-dominated estuarine systems (Trincardi et al., 1994; Amorosi et al., 1999a). The retrogradational stacking pattern of thin transgressive shoreface deposits (Rizzini, 1974; Amorosi et al., 2005) is associated with backstepping bay-head deltas that represent the forced landward shifts of fluvial river mouths under rapid, stepwise sea-level rise (Dalrymple et al., 1994; Boyd et al., 2006 – Fig. 7B). The ravinement surface (Fig. 8C, D), a characteristic erosional surface overlain by a veneer of mollusk-rich sands, separates back-barrier deposits from overlying offshore muds and has a strong lithologic expression. Millennial-scale parasequences (Amorosi et al., 2005; Stefani and Vincenzi, 2005), 3–5 m thick, are retrogradationally stacked as valleys were backfilled, bayhead deltas being confined to flooded river valleys (Fig. 7B).

## 7.2. Offshore stratigraphy

The Late Pleistocene–Holocene TST formed during a phase of rapid, but not monotonic sea-level rise between ca. 18 to 6 cal kyr BP (Asioli, 1996; Bard et al., 1996), and resulted in a complex depositional architecture compared to the short time interval encompassed (Cattaneo and Trincardi, 1999). At regional scale, the TST comprises three main "correlative records": 1. on the low-gradient North Adriatic shelf, it is

composed of patchy, backstepping barrier islands and discontinuous incised-valley systems (Correggiari et al., 1996a,b; Storms et al., 2008; Taviani et al., 2015; Fig. 10), with a facies arrangement similar to the TST preserved landward of the modern coastline (see Section 7.1 and Fig. 9); 2. in the MAD slope basin, it consists of a continuous marine succession (Asioli et al., 1999, 2001); whereas, 3. on the Central Adriatic shelf, it is a composite fine-grained sediment body, >25 m thick, consisting of subaqueous progradational deposits that can be divided into three main units separated by two prominent surfaces (S1 and S2 surfaces, Cattaneo and Trincardi, 1999; Maselli et al., 2011; Fig. 9). PRAD2–4, in 54 m water depth on the shelf West of the MAD, cored 32 m of Holocene deposits, down to the upper portion of a mid-TST progradational unit, beneath erosional surface S2, deposited during the Younger Dryas cold reversal (Piva et al., 2008c; Vigliotti et al., 2008; Maselli et al., 2011).

Located between the northern shelf (where the TST is thin and discontinuous) and the Central-Adriatic shelf (with an expanded and complex TST record), the 260-m-deep MAD slope basin offers a continuous marine record of transgressive deposits, where century-scale chronological control by <sup>14</sup>C dating is supported by the correlation of foraminiferal ecozones and pollen spectra (Calanchi et al., 1998; Asioli et al., 1999, 2001; Blockley et al., 2004). Moreover, geochemical analysis of late Quaternary marine deposits allowed us to compare fine ash layers within Adriatic sequences to tephra layers (dating both by radio-carbon and varve chronology) preserved in Lago Grande di Monticchio (South Italy), and allow corrections for changes in the marine reservoir that occurred through the last deglaciation (Lowe et al., 2007).

The complex internal geometry of the Central-Adriatic TST reflects the interaction between sea-level rise, lateral changes in sediment delivery, advection by marine circulation and pre-existing sea-floor morphology. Seismic-stratigraphic interpretations, integrated with dated samples along the Central Adriatic shelf, correlated to the deepest part of the basin (core CM92-43; Asioli et al., 2001), indicate that the ITST unit beneath surface S1 (Figs. 9 and 10) records the early phases of the last sea-level rise, from –120 and –95 m and the time interval between ca. 18 kyr and 14.5 cal kyr BP (Cattaneo and Trincardi, 1999). This unit develops in continuity with the Po lowstand delta, being characterized by a markedly aggradational geometry in the topset region compared to the underlying delta. During this interval of time, the basin was still characterized by cold-water planktonic species, like *Globigerina bulloides* and *Globigerina quinqueloba*, and was influenced by the fresh water inputs of the Po and other Apennine rivers, as indicated by the presence of the benthic species *A. perlucida* (Asioli, 1996). The middle TST unit (mTST), between surfaces S1 and S2, records sea-level rise between –95 and –60 m, and consists of a composite prograding wedge, thicker than 10 m on the shelf, and by a continuous unit of marine mud in the MAD slope basin. Stratigraphic correlations to core CM92-43 and the recognition of tephra C-2 and Y1 in core PAL94-8 (Calanchi et al., 1998) indicate that surface S1 was older than 14.5 cal kyr BP (Cattaneo and Trincardi, 1999). The upper TST unit (uTST), confined between surface S2 and the mfs, records the last phases of sea-level rise, starting at about –60 m. This unit is composed of marine muddy sediments (Fig. 9) and shows two main shore-parallel depocenters, suggesting a mechanism of sediment dispersal similar to the modern one (Cattaneo et al., 2004). The upper TST unit is composed of marine mud, rich in planktonic foraminifera with assemblages typical of an outer-shelf to upper-slope environment. Dated samples show that the upper TST unit covers the period following Meltwater pulse 1B (ca. 11.5–11.1 kyr cal BP, Bard et al., 1996) including the interval of hydrological reorganization of the Mediterranean that led to the deposition of Sapropel S1 (Maselli et al., 2011, 2014).

The mTST unit, between erosional surfaces S1 and S2, was deposited offshore between Meltwater Pulses 1A and 1B, recording an interval of increased sediment flux from land and a possible sea-level stillstand, or minor fall (Cattaneo and Trincardi, 1999; Maselli et al., 2011). The mTST unit defines four main depocenters, elongated parallel to the

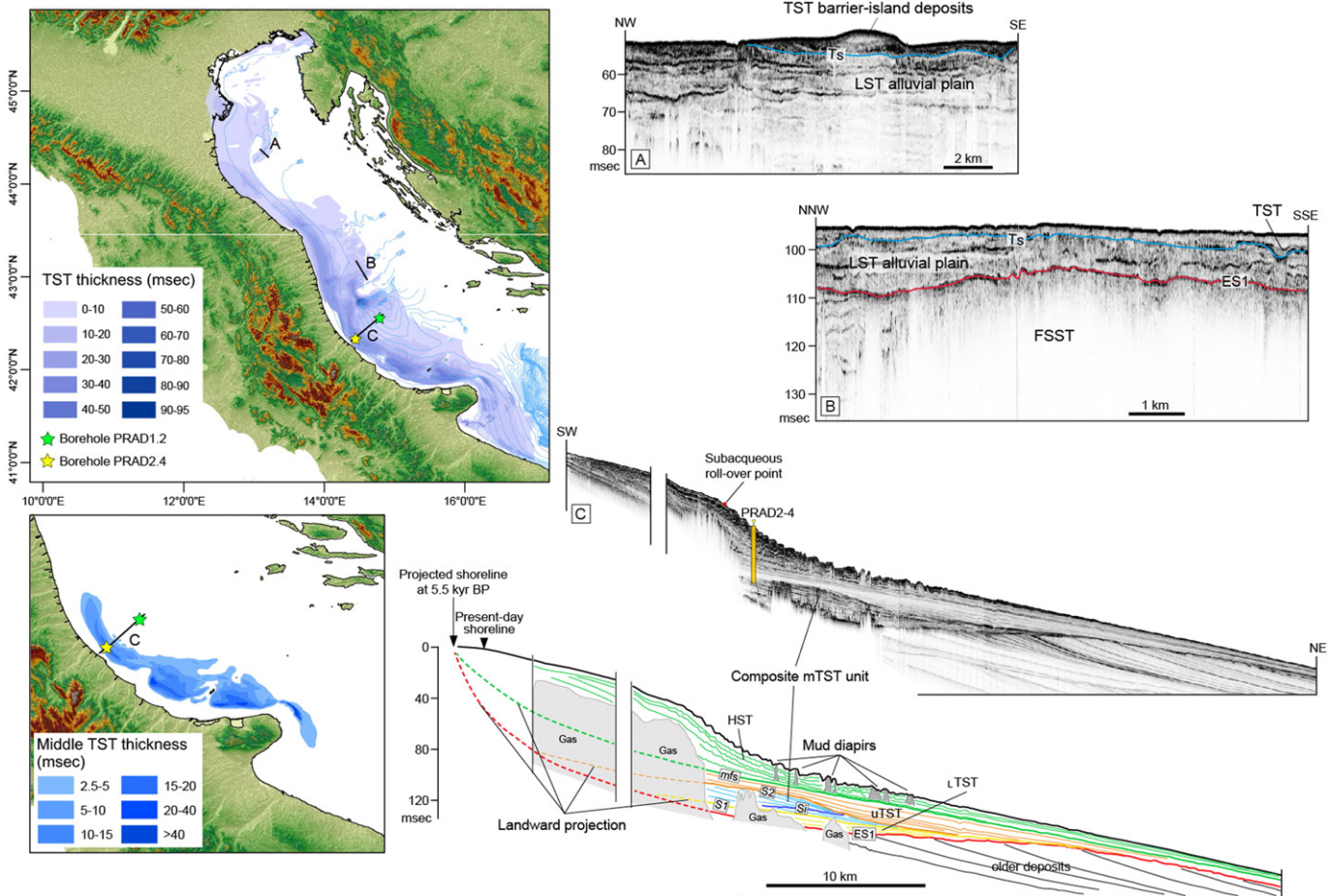


**Fig. 10.** Thickness distribution of the coastal-marine component of the late-Quaternary TST (18–5.5 kyr BP). The thickness of the middle-TST unit is reported in the inset below, and the composite nature of this unit is depicted in the seismic profiles of the Central Adriatic shelf. The unit between surfaces S1 and S2 records the Younger Dryas cold spell in the form of a rapid and short-lived regressive interval. As a whole, the thickness distribution of the m-TST unit reflects a significant component of shore-parallel sediment dispersal. In the northern Adriatic shelf the TST occurs in patches of sandy coastal lithosomes variably reworked after drowning in place.

coast, reflecting local deltaic entry points and alongshore-oceanographic currents (Cattaneo and Trincardi, 1999; Pellegrini et al., 2015; Figs. 9 and 10). The effect of alongshore sediment dispersal is particularly evident in the southernmost depocenters, East of the Gargano Promontory, where a subaqueous delta was deposited (Pellegrini et al., 2015). In all four areas, the mTST unit is 10–15 m thick in the middle shelf, pinching out offshore, and includes heterolithic facies with sharp-based sandy layers; two prograding bodies (mTST-1 and mTST-2 sub-units) are separated by an internal unconformity (surface S1, Fig. 10); the mTST-1 sub-unit is composed by low-angle, seaward dipping reflections, with direction of progradation oblique to the coast, while mTST-2 sub-unit, > 8 m thick, is located more landward and shows higher-angle downlapping reflections, prograding beyond the limit reached by the mTST-1 sub-unit, and is eroded at the top.

## 8. Highstand systems tract (6 cal kyr BP to Present)

### 8.1. Onshore stratigraphy

The maximum flooding surface (MFS) marks the inversion from a retrogradational to a progradational facies architecture (Fig. 7B). This surface, which developed when sediment supply exceeded the rate at which accommodation was created, exhibits distinct characteristics in the different portions of the Po Plain. Beneath the modern delta and in the coastal area, it correlates with a condensed fossiliferous horizon within shallow-marine deposits, recording prolonged storm winnowing

(Amorosi and Marchi, 1999; Stefani and Vincenzi, 2005). In back-barrier positions, the MFS coincides with bay or lagoonal deposits rich in *Cerastoderma glaucum* sandwiched between freshwater swamp, organic-rich clay (Fig. 8E). Within non-marine facies, the up-dip expression of the MFS is traced at the base of laterally extensive paludal and poorly drained floodplain horizons within a thick Holocene succession of continental deposits (Fig. 7A).

The early highstand phase saw the development of large sand spits and barrier islands that turned the previous bays into confined lagoons (Stefani and Vincenzi, 2005). During this phase, aggradation took place in subsiding delta plain environments (Fig. 7A), progradation was restricted to bay-head delta positions (Amorosi et al., 2003), while prolonged condensation (about 8 to 5.5 cal kyr BP) is recorded within offshore deposits (Scarpioni et al., 2013).

The stratigraphic architecture of the upper HST can be reconstructed in detail, since coastal sediments crop out and generally preserve their primary geomorphic form (Stefani and Vincenzi, 2005). Accurate reconstruction of drainage network evolution and delta development during the late Holocene has been enabled by detailed geomorphological studies, which showed a diachronous array of distributary channels feeding a series of sub-parallel beach ridges (Ciabatti, 1967; Veggiani, 1974; Sgavetti and Ferrari, 1988; Bondesan et al., 1995; Castiglioni et al., 1999; Stefani and Vincenzi, 2005). During a prolonged phase of its early growth, the Po Delta was a wave-dominated system (Galloway, 1975), with delta front arcuate ridges laterally connected to prograding strandplains, made up of rectilinear beach ridges with associated aeolian sands (Stefani and Vincenzi, 2005). Delta progradation

is reflected by the vertical transition from prodelta muds to nearshore sands (Fig. 11A), showing the characteristic vertical succession of offshore-transition, lower shoreface and upper shoreface/foreshore facies associations (Fig. 7B – Rizzini, 1974; Amorosi et al., 1999a). In more internal position, delta front sands are replaced by lagoonal (lower delta plain) and swamp (upper delta plain) facies (Figs. 7B and 11B). This shallowing-upward succession is capped by transition to alluvial deposits (Fig. 11C).

The Etruscan and Roman times were characterized by a warm climate and by riverine stability associated with the development of a large delta lobe south of Ferrara (Stefani and Vincenzi, 2005). At around 1500 yr BP, the transition toward moister and cooler conditions and the demise of the Roman Empire infrastructure led to widespread flooding and drainage network instability (Stefani and Vincenzi, 2005; Bruno et al., 2013). The historical Po River avulsion in 1152 AD, close to the Ficarolo village, shifted the Po Delta system toward the present-day fluvial axis (Veggiani, 1974; Bondesan et al., 1995). The complex history of distributary channel avulsion and delta lobe abandonment, reflecting an overwhelming autogenic control on sedimentation, is recorded by the common alternation of swamp and floodplain deposits within the HST (Fig. 7A), which is chronologically well constrained on the basis of archeological data (Fig. 11C).

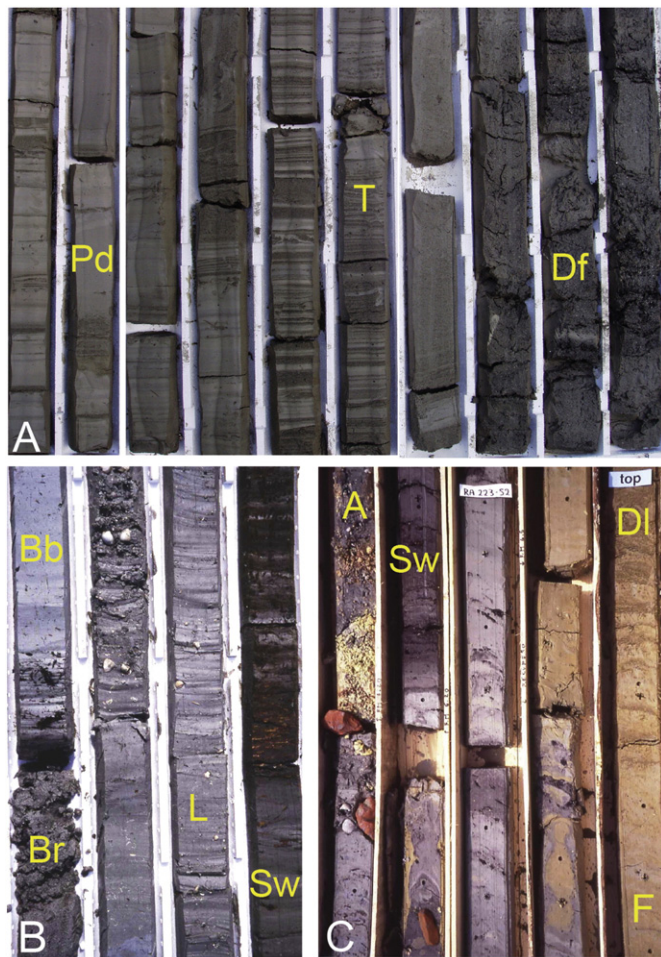


**Fig. 11.** Representative core photographs from the subsurface of the Po Plain, depicting vertical stacking of highstand (HST) facies associations A: shallowing (and coarsening) - upward succession of prodelta (Pd) to delta front (Df) deposits (T = transitional facies) beneath the modern Po Delta. B: shallowing-upward succession of beach-ridge (Br), Back-barrier (Bb), lagoonal (L) and coastal swamp (Sw) deposits in more internal position (lower HST). C: upward transition from swamp (Sw) facies to floodplain (F) and distal levee (DL) deposits (upper HST). A indicates artifacts of Roman age that were accidentally encountered during coring operations. Core bottom is lower left corner. Core width is 10 cm.

The modern, cuspatate delta lobe was human induced at the beginning of the 17th century (1604), when an intervention by the Republic of Venice forced the Po to flow southward through an artificial fluvial mouth (Correggiari et al., 2005b; Stefani and Vincenzi, 2005; Maselli and Trincardi, 2013b). This delta very rapidly prograded, forming a strongly protruding delta under exceptionally high depositional rates, with 20 km of progradation taking place in just 120 years (Stefani and Vincenzi, 2005).

## 8.2. Offshore stratigraphy

The highstand systems tract encompasses a thin wedge-shaped prodelta deposit offshore of the North Adriatic coastal plain, and related minor deltas and lagoons (Cattaneo et al., 2007), a markedly progradational prodelta wedge offshore of the Po River delta (Correggiari et al., 2005a) and Apennine coast (Cattaneo et al., 2003). In Fig. 12 all profiles are reported at the same horizontal scale and vertical exaggeration documenting that the largest accumulation occurs southward of the modern Po River delta, with a prodelta wedge that reaches a thickness up to 35 m under the effect of shore-parallel sediment transport for about 600 km along the Adriatic coast of Italy, until the Gargano Promontory where it forms a subaqueous delta (Cattaneo et al., 2003, 2007). The HST is floored by the MFS, a regional and prominent downlap surface that can be traced on seismic profiles over a distance exceeding 600 km, from the Po Delta to the region surrounding the Gargano Promontory (Fig. 5). The sedimentologic expression of the MFS in marine cores is subtle and may consist of a firm ground (accompanied by discernible increase in strength in pocket penetrometer and in shear-stress resistance tests – Canals et al., 2004; Sultan et al., 2008). In places, mollusks exploit the stiffer character of the sea floor with the establishment of Oyster communities and Bryozoans pavements (Sultan et al., 2008). From a micropaleontological perspective, the MFS is approximated by the Last Occurrence of the planktonic foraminifer *G. inflata*, dated by  $^{14}\text{C}$  to 5500 years BP (Asioli, 1996; Piva et al., 2008c). The condensed section associated with the MFS varies from a few hundred years in the Gargano area (Oldfield et al., 2003) to several thousand years beneath the modern Po River delta.

The key characters of the Modern Po Delta are a) the marked asymmetry of the entire delta-prodeltal system, reflecting the prevailing sediment dispersal to the south of each individual delta outlet, as observed in other deltas (Bhattacharya and Giosan, 2003); b) the shore-parallel overlap of successive prodelta lobes fed by distinct river outlets of ever changing relative importance; c) the delta outlets being artificially forced in a fixed position, so that natural avulsion is prevented and delta lobes undergo headland retreat experiencing marked erosion on the prodelta topset (Trincardi et al., 2004). The seismic stratigraphy of the Modern Po Delta shows that markedly distinct prodelta architecture may form depending on where the newly activated lobe is located: when the new lobe is updrift (north, in this case) of the one that is retreating, the abandoned lobe becomes sheltered by the new rapidly advancing one; in the opposite case, when the new lobe is downdrift (South) of the one that is retreating, a substantial portion of the retreating updrift lobe, is cannibalized and transported to the new lobe (Correggiari et al., 2005b).

On seismic profiles perpendicular to the coast, the Adriatic shelf clinoform shows foresets dipping typically 0.5 to 2° within elementary sigmoidal units (Cattaneo et al., 2003; Fig. 5). A prominent morphologic feature is the subaqueous “rollover point” (Steckler et al., 1999; separating topset and foreset strata) in about 25 m water depth; this diagnostic feature can be traced approximately 350 km along the coast North of Gargano Promontory. As suggested by direct dating on the basal surface and interpolations of sediment accumulation rates derived from short-lived radionuclides ( $^{210}\text{Pb}$ ), the most recent portion of the clinoform deposited during the last 500 years (Cattaneo et al., 2003; Correggiari et al., 2005b; Frignani et al., 2005; Palinkas et al., 2005), an interval encompassing the Little Ice Age. Offshore of the

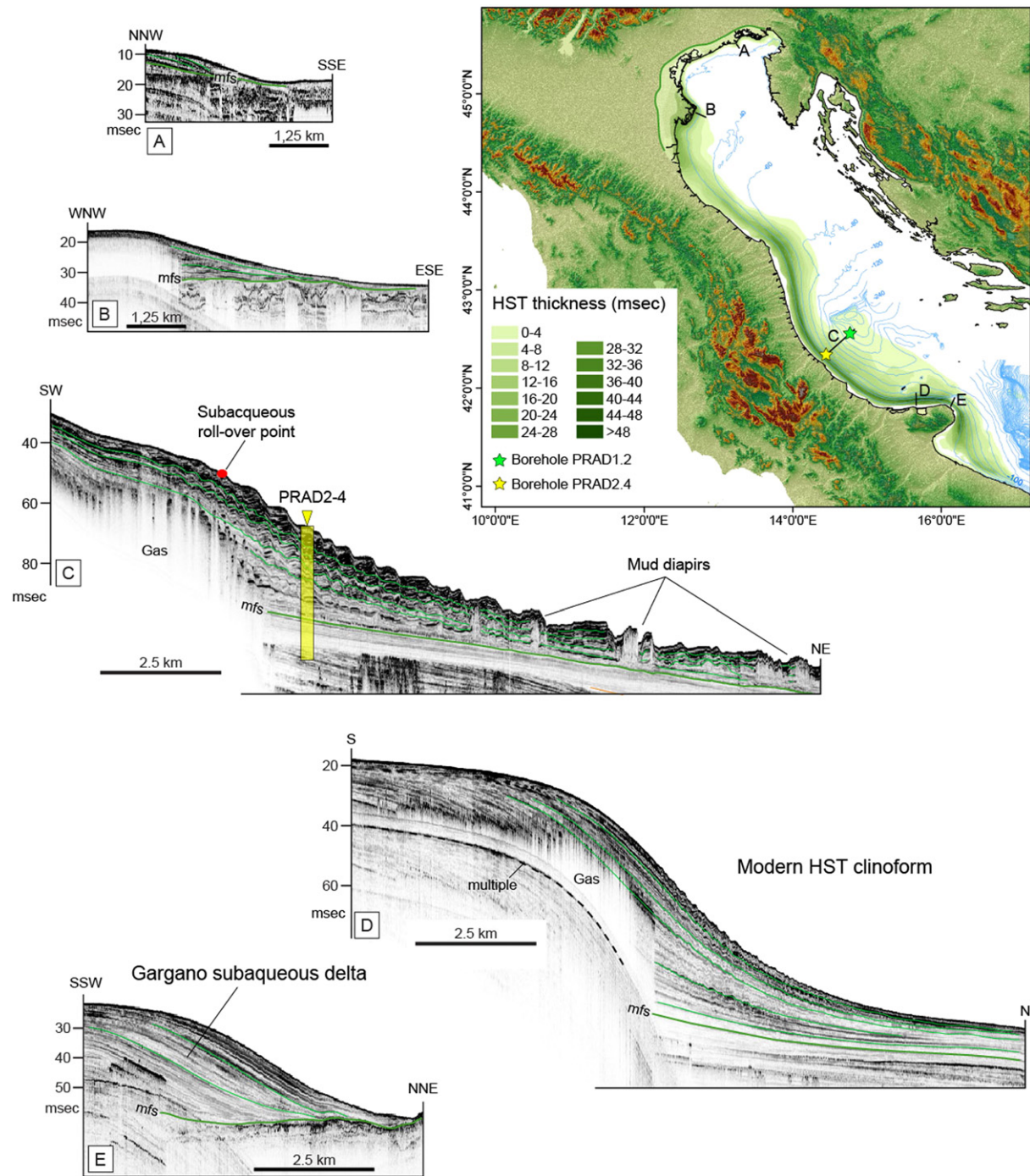


**Fig. 12.** HST stratigraphy from the North Adriatic shallow shelf (Tagliamento delta, upper left) to the Po and proceeding south to the Central Adriatic, the Gargano Promontory. Note that all profiles are displayed at the same horizontal scale and vertical exaggeration (ca. 80×), showing how the Po delta (the most prominent delta plain of the basin) has rather small sediment volume compared to the subaqueous clinoform. The seaward downlap of the clinoform on the MFS increases in steepness proceeding south, indicating enhanced interaction between bottom currents and pre-existing coastal and shelf morphological constraints.

Gargano Promontory, where the interaction between shore-parallel southward flowing currents and basin morphology is at its maximum, the clinoform advances onto a flat bedrock in about 50–80 m water depth (Fig. 12). The rapid cross-shelf wedging out of muds from 30 to 0 m is a good indication of the role played by southward-flowing, bottom-hugging currents that prevent deposition in the bottomset and cause sediment transport along strike.

The foresets of the Adriatic clinoform are actively forming, as documented by the progressive seaward shift in the area of active deposition through time and may preserve flood event beds or appear pervasively bioturbated (Fig. 9). Furthermore, the thickness distribution within the

clinoform over different time scales is elongated parallel to the western Adriatic coast testifying to the importance of southward sediment transport. One of the major findings about clinoform generation from the EURODELTa and EUROSTRATAFORM projects is that present sediment transport is sub-parallel to the foreset strike, with a likely slight offshore component that allows active outbuilding basinward (Nittrouer et al., 2004; Sherwood et al., 2004; Frignani et al., 2005; Palinkas et al., 2005; Puig et al., 2007; Cattaneo et al., 2007). Comparison of seismic stratigraphic records and sediment-accumulation rates over the last century (based on short-lived radionuclide data) shows that the largest absolute accumulation rates are encountered at the extreme tips of the

systems, offshore of the Po Delta and just updrift of the Gargano Promontory, while the offshore component of dispersal is greater in areas of flow divergence located downdrift of the Gargano Promontory (Cattaneo et al., 2003, 2004, 2007; Taviani et al., 2012).

An important character of the Adriatic shelf clineform is the variability of bottomset-tapering basinward. The usual assumption explaining clineforms is that the topset reflects near-bed shear stress and sediment bypass (Nittrouer et al., 2004; Sherwood et al., 2004); in the foreset, shear stress decreases and sediment accumulation is at a maximum, while in the bottomset, less sediment is available and sediment accumulation decreases for this reason alone. In the case of the Adriatic, however, the clineform grows basinward and tapers out seaward, not simply because sediment is trapped in the foreset region, but because the bottom current intensifies and prevents sediment accumulation on the bottomset (Cattaneo et al., 2007). The Adriatic example shows therefore that the growth of a clineform can be energy limited (as off the Gargano Promontory): this is the result of shore-parallel currents like those related to the southward flow of the NADDW dense shelf water, which increase energy in the bottomset, preventing deposition or reworking sediment.

## 9. The Po Plain–Adriatic system: a source-to-sink approach

Reconstructing sediment transfer from the source area to the final sink represents an intriguing application of sequence-stratigraphic concepts. In the late Quaternary succession of the Po Plain–Adriatic system, shoreline trajectories unambiguously reflect sea-level changes,

and are correlative landwards and seawards to consistent changes in alluvial and marine facies architecture, respectively. The resulting stratigraphic model, thus, can provide constraints to interpret and predict sedimentary basin architecture of older successions potentially governed by relative sea-level change, with special emphasis on facies patterns, sediment body dimensions and connectivity.

Despite the abundance of stratigraphic studies conducted on its individual segments, a comprehensive sequence-stratigraphic framework for the entire Po Plain–Adriatic system is still lacking. The large body of data summarized in the previous sections allows for the first time a system-scale analysis to be completed, for the LGM and post-LGM intervals of time, i.e. the last 30 kyr.

### 9.1. Key stratigraphic surfaces

Although key controls of stratigraphic architecture, such as accommodation and sediment supply varied through space and time across the Po Plain and the Adriatic Sea during the last glacial–interglacial cycle in response to predominantly local factors, the entire dispersal system responded in a largely contemporaneous manner to the overwhelming control by sea-level and climate change. In this context, the key stratigraphic surfaces potentially useful for regional correlations can be tracked physically across the sediment routing system, and allow tentative reconstruction of ancient landscapes (Fig. 13).

Most of the key surfaces recognized can be traced over several hundreds of km from the upper continental slope to the inner coastal plain; radiometric constraints across these surfaces are highly consistent

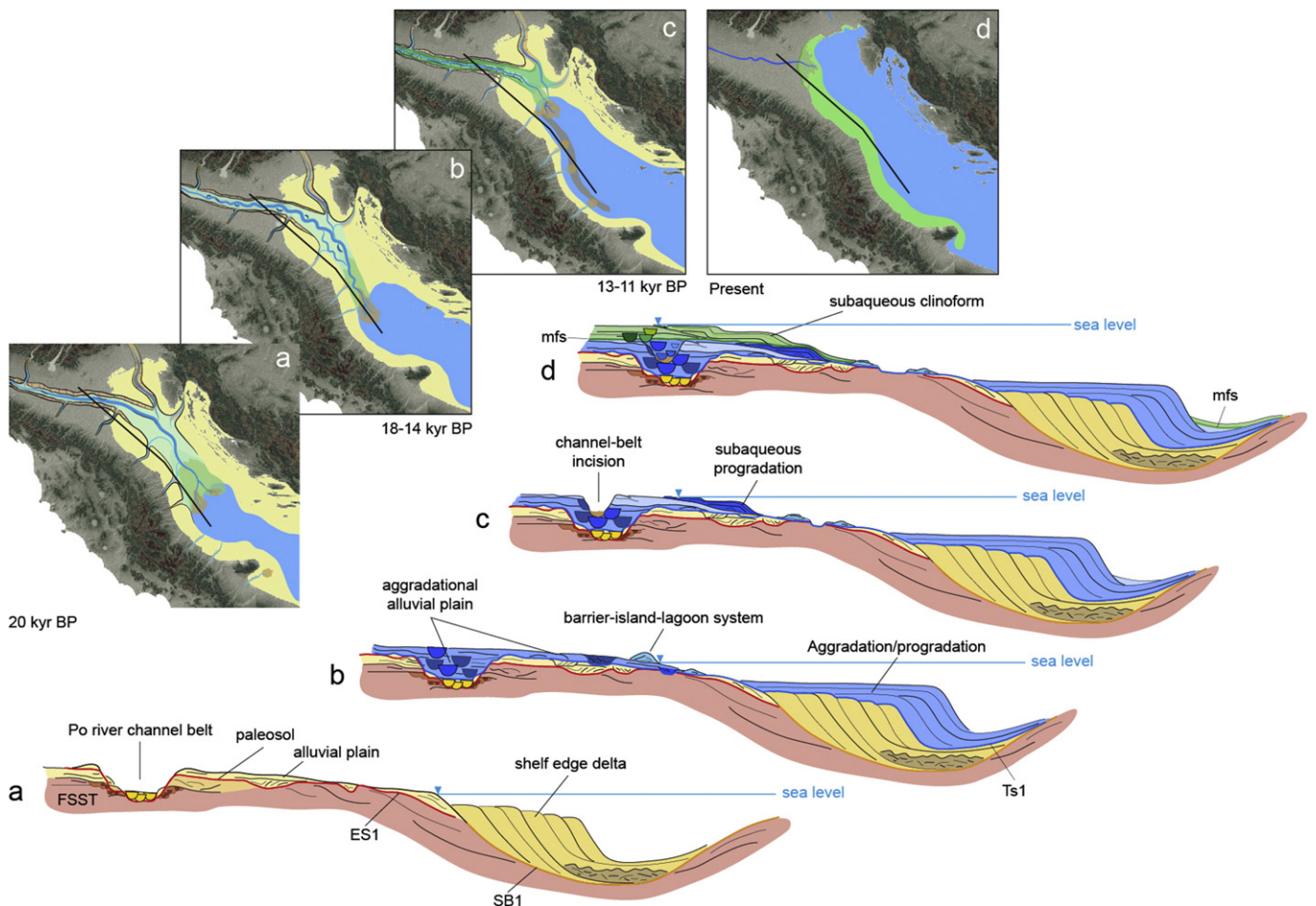


**Fig. 13.** Sedimentary evolution of the Po Plain–Adriatic basin, and related stratigraphic architecture, for the last 20 kyr: at lowstand times (a), early transgression (b), middle transgression (c), and at present (d). Note that the scale of the channel belt deposits in the Po plain is emphasized compared to that of the shelf-edge delta; the subaqueous progradation onsets during mid TST times indicating the establishment of an oceanographic circulation similar to the modern one.

over the entire study area, providing the basis for the reliable reconstruction of paleoenvironmental evolution from the continental to the deep marine realms. Where sedimentation is continuous and “expanded”, the following surfaces can be identified and traced:

- a. Sequence Boundary (SB): is represented by an Inceptisol, at the top of a series of closely-spaced paleosols, that correlates laterally to an extensive channel-belt sand body fed by the Po River, and to smaller-sized incisions formed by its Apennine tributaries (Fig. 7). The SB is typically an erosional unconformity on the entire continental shelf, locally with significant plurimetric relief, such as in the outer-shelf region offshore of the Tremiti Island, where it tops a well preserved FSST (Trincardi and Correggiani, 2000);
- b. Transgressive Surface (TS): exhibits markedly different facies characteristics across the distinct segments of the system, sharing a diagnostic (glacial to interglacial) pollen signature (Amorosi et al., 2004). In the coastal plain, the TS is marked by the sharp facies contrast from well-drained, floodplain deposits (LST) to organic-rich, paludal and estuarine deposits. Offshore, the TS is marked by either a sudden drowning of the shelf or the onset of a more aggradational stacking pattern atop the Po LST.
- c. The Younger Dryas unconformity (YD): corresponds to a highly continuous, weakly developed paleosol horizon that can be traced throughout the Po Plain, from its southern margin to the Adriatic Sea. On land, this stratigraphic unconformity may coincide with the TS (Fig. 7). Its correlative fluvial bodies are small-sized and patchily distributed. Offshore, the YD becomes a subaqueous erosion surface, with marked truncation of the underlying, prograding oblique reflectors. The YD mimics the SB geometry, though time scales and geometries of middle TST and LST differ by one order of magnitude.
- d. Ravinement Surface (RS): though highly diachronous (Saito, 1994), it is a readily identifiable surface, marking a sudden (litho)facies change from back-barrier to transgressive shoreface deposits and from offshore sand to mud. The Central Adriatic area records interesting examples of offshore RS, where a marked erosional surface separates marine deposits with comparable facies above and below (Maselli et al., 2011; Fig. 9).
- e. Maximum Flooding Surface (MFS): marks an interval of condensed deposition generally greater than 2500 years (Scarpioni et al., 2013), with marked change from backstepping to progradational depositional geometries. In core, the MFS represents the turnaround from deepening-upward to shallowing-upward trends across a variety of depositional systems. Offshore, depending on local conditions of sediment supply, topographic gradient and rate of relative sea-level rise, the MFS may coincide with the TS (Trincardi et al., 1994; Cattaneo and Steel, 2003). Where the TST is lacking or non-preserved, all surfaces related to relative sea-level rise (TS, RS and MFS) coincide.

## 9.2. Paleoenvironmental evolution

Stratigraphic data argue for a significant role of the axial drainage system in the paleoenvironmental evolution of the Po Plain–Adriatic system, with a trunk channel (the Po) acting as collector of tens of tributaries from the Alpine and Apennine chains, by transit back and forth across the Adriatic shelf (Maselli et al., 2011). When sea level reached its lowest position, 120 m below present sea level, the northern Adriatic was almost entirely subaerially exposed, and the Po River almost doubled its present length, greatly enlarging its drainage basin by incorporation of the eastern Alpine river catchments (Fig. 1).

The last important phase of Quaternary sea-level fall recorded at the MIS3–MIS2 boundary, combined with the abrupt climate change to fully glacial conditions (LGM), forced channel incision in the axial part of the system, promoting the formation of a major channel belt fed by the Po

River. Coeval episodes of fluvial valley incision have also been documented from several coeval coastal plain successions (Dabrio et al., 2000; Wellner and Bartek, 2003; Busschers et al., 2007; Blum et al., 2008; Kasse et al., 2010; Amorosi et al., 2013a). Fluvial incision was followed during the LGM by lateral migration, valley widening, and fluvial deposition under lowstand conditions, leading to the formation of a 30 m-thick channel-belt sand body, up to 20 km wide (Fig. 13a). There is scattered evidence of smaller-sized (<10 m deep), coeval fluvial incisions by the Apenninic tributaries, in response to base-level fall by axial fluvial incision.

Despite high-density of seismic investigation, there is no clear indication of thick and wide channelized bodies of comparable size, in the central Adriatic. We are not able, at present, to reconstruct precisely lowstand sand pathways through the whole dispersal system. It is likely, however, that the Po River system became distributive in the central Adriatic area, in response to extremely low shelf gradients; through this complex distributive system, made up of narrow and linear, small-sized valleys, the Po channel belt was feeding and genetically linked to the prograding lowstand delta (Fig. 13a).

Aggradational (onshore) to progradational (offshore) stacking patterns define the lowstand systems tract across the Po Plain–Adriatic system. Transgressive and highstand depositional regimes differ substantially from the lowstand sediment distribution system. An obvious change from progradational to retrogradational stacking patterns, assigned to the Meltwater Pulse 1A (Fairbanks, 1989; Bard et al., 1990, 1996), characterizes the lower and middle TST in the Adriatic (Fig. 13b). The lower TST north of the MAD slope basin developed atop the LST delta, from which it is separated by a prominent surface (TS) marking the onset of significant topset aggradation, while sediment flux from the continent was sufficient to maintain margin progradation. The onshore equivalents of the early transgressive deposits recognized offshore are, instead, represented by thin aggradational, non-marine deposits that are recorded patchily within the latest Pleistocene valley systems (Fig. 13b). We remark here the importance of antecedent topography created during falling sea-level on shaping the nature of transgressive deposits during the ensuing sea-level rise (Simms and Rodriguez, 2014).

The prograding transgressive unit recognized through high-resolution seismic profiles in the Central Adriatic (middle TST unit of Cattaneo and Trincardi, 1999; Maselli et al., 2011) marks a significant change in sediment supply regime (Fig. 13c). This unit, which records a period of extreme climatic instability (including the Younger Dryas climate event) between about 14.8 and 11.3 cal kyr BP, is largely correlative with the nearly coeval (13.5–11.6 cal kyr BP), laterally extensive paleosol recently identified in the subsurface of the Po Plain (Amorosi et al., 2014 – Fig. 13c), and is tentatively related to a minor sea-level fall (Maselli et al., 2011). Enhanced sediment flux during the Younger Dryas has also been reported by Abdulah et al. (2004) and Anderson et al. (2004), and from several European margins (Hernández-Molina et al., 1994; Berné et al., 2007; Amorosi et al., 2013b).

The Younger Dryas paleosol, and its genetically related, prograding wedge offshore mimic, at the millennial scale, the sequence boundary and its related lowstand delta. Owing to its short-lived nature, there was insufficient time for a well developed channel belt to form, and fluvial deposition at that time appears to be restricted to small-sized channels, locally re-incising the lowstand channel belt (Fig. 13c).

The Holocene sea-level rise, starting with Meltwater Pulse 1B, is clearly reflected by the rapid backstepping of barrier-lagoon-estuary systems, which is observed first (between 11,500 and 9000 cal kyr BP) in the northern Adriatic (Trincardi et al., 1994; Correggiani et al., 1996a) and subsequently (between about 9000 and 8000 cal kyr BP) in the Po Plain (Amorosi et al., 1999a, 2003, 2005). Backstepping shoreface bodies are recorded up to 20 km inland of the present-day shoreline position (Fig. 7B).

The maximum landward migration of the shoreline took place around 7800 cal kyr BP. Stratigraphic condensation at the turnaround

between deepening-upward (TST) and shallowing-upward (HST) trends (maximum flooding surface) is marked by a fossil-rich horizon, where within-bed depositional resolution is lowest and age mixing is commonly around 2500 years (Scarpioni et al., 2013). This observation is consistent with radiometric dating from early highstand deposits, which record Po delta progradation starting around 5500–5000 cal yr BP (Asioli, 1996; Oldfield et al., 2003; Piva et al., 2008c; Amorosi et al., 2005).

Aggradation of alluvial-plain deposits and delta progradation are the most typical feature of the HST (Fig. 13d). In general, highstand architecture reflects a variety of processes, sea-level control is strongly subdued and autogenic processes, together with climate change, appear to be the dominant driving mechanisms.

## 10. Sediment budget

### 10.1. Approach

Estimating sediment budgets in ancient basins is a difficult task, hindered, in most cases, by a loose control on the paleogeographic setting, lack of continuity in source-to-sink correlations and, in some cases, the need to integrate knowledge from investigations that range from outcrop-scale studies to full 3D seismic volumes.

Late Quaternary systems, like the Po Plain–Adriatic basin, have higher potential for sediment budget estimates, and may permit an evaluation of source-to-sink controls at millennial scales (Romans et al., 2009), but yet the exercise is not trivial. Prodeltal sediment budget analysis from the Adriatic Sea has been attempted by Brommer (2009), Brommer et al. (2009), and Weltje and Brommer (2011), who derived mass-accumulation rates by means of stochastic simulation, using high-resolution seismic data, porosity profiles, and radiocarbon dating. Based on refined sequence-stratigraphic analysis and basin-scale correlations, we propose here an estimate of the sediment volume stored in each systems tract, with decreasing level of uncertainty from the LST to the HST. For each systems tract we tried to estimate for the first time the spatial partition of bulk sediment into distinct sedimentary environments: fluvial-channel belt, alluvial/coastal plain, continental shelf, and shelf edge and beyond. This approach allowed us to define, at least approximately, the shift of the main sediment storage areas across different environments and through time.

Seismic records and mapped systems tracts can be used to infer sediment yield and paleodischarge (Guillocheau et al., 2011). In estimating the systems tract thickness offshore, we proceeded, following Cattaneo et al. (2004), based on the interpretation of conventional, 2D seismic surveys, locally with increased data density giving rise to pseudo-3D data coverage. The thickness of each systems tract was measured in two-way travel time (TWTT) of the P waves. This information can be converted into meters based on assumptions or measurements of the P-wave velocity across the measured section.

Systems tract geometries on land were reconstructed through bore-hole transects. The thickness of individual fluvial storeys as deduced from cross-sections of channel belts was used as proxy for paleoflow depth, which scales to contributing drainage area, relief and sediment yield (Blum et al., 2013; Blum and Pecha, 2014; Holbrook and Wanam, 2014). In the case of the paleo Po, using data extractable from cores, the single-storey value, and thus flow depth, is about 10 m (Fig. 7). This value was used for volume calculations to separate the lowstand channel-belt sand body from the underlying, locally amalgamated older channel belts, assigned to the FSST.

All volumes were extrapolated following basin-scale correlations, through GIS-assisted mapping. Sediment volumes were then converted to mass estimates, adopting a conversion factor of  $1.8 \text{ m}^3$ . Sediment volumes within the three systems tracts were also divided by the time duration of each systems tract (LST = 12 kyr, TST = 12 kyr, HST = 6 kyr). This was done, in a first approximation, by assuming constant accumulation rates within each systems tract, thereby inevitably

smoothing the possible impact of higher-frequency sea-level or climatic fluctuations.

On much shorter time scales, and in the last few decades, an independent estimate of mass accumulation rates was derived from sediment (and mass) accumulation rates measured by short-lived radionuclides, typically on scales from months ( $^{7}\text{Be}$ ) to a century ( $^{210}\text{Pb}$ ) and compared to the values averaged over longer-term intervals.

We are aware that sediment budget calculations that fail to assess the specific contribution of distinct source areas to the total sediment volumes may create unrealistic estimates of sediment flux. In this respect, the estimates illustrated in the following sections should be regarded as a first approximation to sediment budget analysis in the Po–Adriatic system. Sediment provenance studies on land related to the late Quaternary succession (Marchesini et al., 2000; Amorosi, 2012; Amorosi and Sammartino, 2014) have recently shown that changes in sediment dispersal patterns can be tracked confidently down to the facies tract scale, and that lithologically homogeneous sediment bodies may hide a much more complex sedimentary history than one could expect. In a multi-sourced sedimentary succession, such as the Po Plain–Adriatic system, fingerprinting the individual facies associations on the basis of their petrographic and geochemical attributes, and its combination with high-resolution sequence stratigraphy may greatly assist in reconstructing sediment pathways. This approach appears as a promising future research direction for the reliable assessment of source-to-sink fluxes and sediment budgets.

### 10.2. Systems tract volumes and sediment budget partitioning

A tentative sediment budget for the study area is shown in Fig. 14, where we report our best calculations/estimates of sediment volumes stored, for each systems tract, in the four key segments of the Po–Adriatic source-to-sink system: (i) the fluvial channel belts, (ii) the floodplain and the adjacent coastal plain (including estuarine – TST – and deltaic – HST – environments), (iii) the continental shelf, and (iv) the shelf to slope-basin setting. A major uncertainty in volume estimates for the LST stems from lack of knowledge in the eastern side of the basin, beyond the midline. Based on paleogeographic reconstructions of the drainage (Kettner and Syvitski, 2008; Maselli et al., 2011), conservative estimates for the Po lowstand delta in that part of the Adriatic suggest a volume equal to 50% of the volume measured on the Italian side; this estimate comes from the studies by Ori et al. (1986), who showed the substantial pinch-out of the Plio-Quaternary depocenter beyond the Adriatic midline.

In general, the LST exhibits the largest size, with a total volume of  $770\text{--}880 \text{ km}^3$  (Fig. 14). Most sediment deposition was confined to the huge LGM lowstand delta ( $650\text{--}700 \text{ km}^3$ ), with only minor contribution from the non-marine part of the system (Po channel-belt sand body). No continental-shelf deposits formed in the LST: at that time, an alluvial/coastal plain was located close to the modern shelf edge, thus representing the feeding system for the Po lowstand delta. The TST total volume is  $290\text{--}340 \text{ km}^3$ , including the shelf edge delta that accumulated during the early phases of the post-LGM sea-level rise. Maximum sediment accumulation under sea-level-rise conditions took place on the continental shelf, while lower sediment volumes are recorded landwards and in slope-to-basin settings. Finally, the HST is  $330\text{--}380 \text{ km}^3$ . Contrary to the LST and TST, highstand sediment accumulation is recorded mostly onshore (alluvial aggradation and coastal progradation) and on the continental shelf, with negligible contribution from deep-water settings.

By dividing the total sediment volume by the duration of each systems tract, we obtained the following averaged sediment accumulation rates:

$$\text{HST: } 355 \text{ km}^3/6 \text{ kyr} = 59.2 \text{ km}^3 \text{ kyr}^{-1}$$

$$\text{TST: } 315 \text{ km}^3/12 \text{ kyr} = 26.3 \text{ km}^3 \text{ kyr}^{-1}$$

$$\text{LST: } 825 \text{ km}^3/12 \text{ kyr} = 68.7 \text{ km}^3 \text{ kyr}^{-1}$$

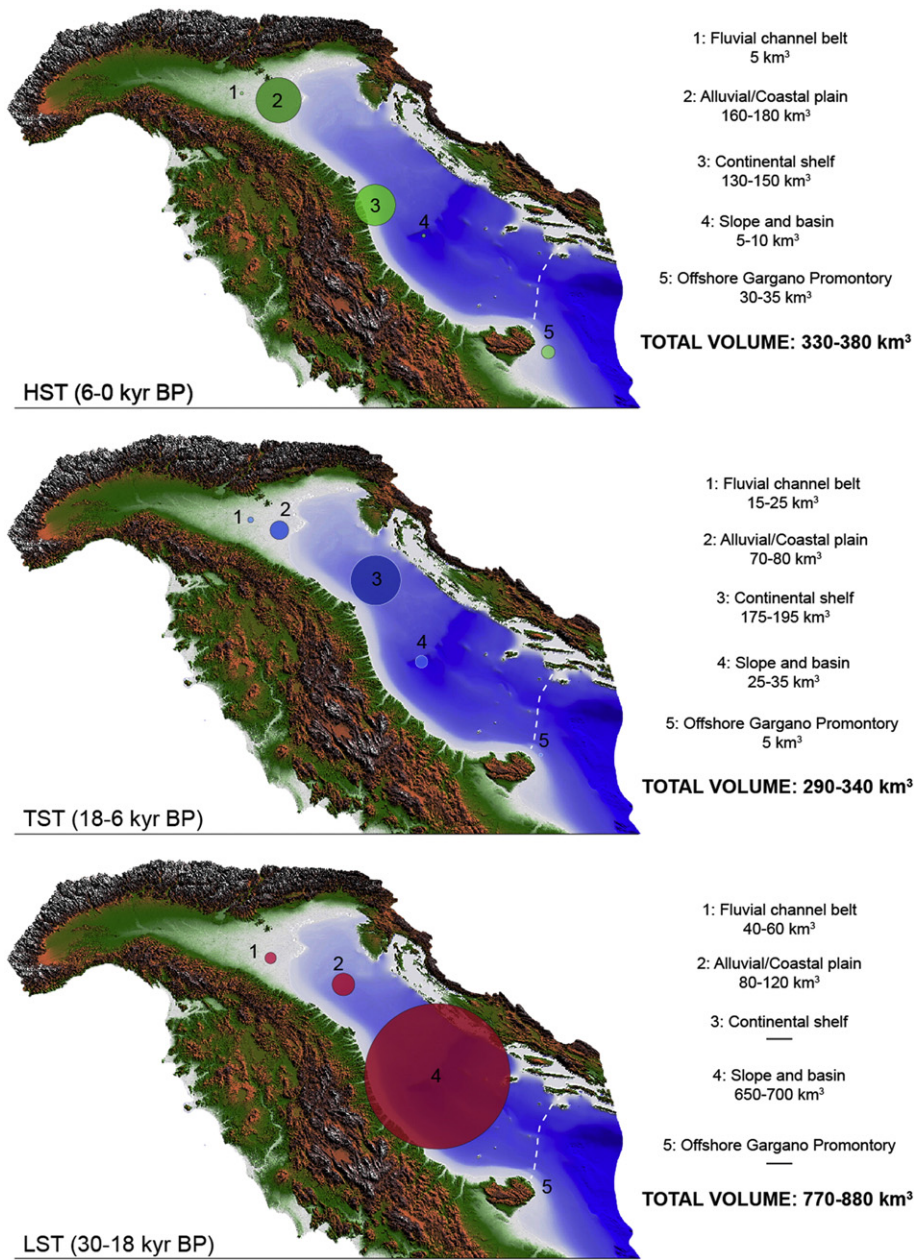


**Fig. 14.** Sediment-budget partitioning across the key segments of the Po-Adriatic source-to-sink system, subdivided by systems tract (LST: lowstand; TST: transgressive; HST: highstand). Uncertainties reflect extrapolations assuming maximum and minimum thickness between two control points. The black horizontal bars in the LST mark the lack of deposition beyond Gargano Promontory and the lack of continental shelf environments in the northern Adriatic when sea level was lowered by 125 m with respect to the modern one and rivers debouched directly into the MAD.

Measurements of modern sediment discharge, though inevitably biased by the pervasive modifications of the environment caused by the anthropogenic impact, provide an independent check of the above calculations, and prove the consistency of our approach. Taking a density of 1.8 t/m<sup>3</sup> and multiplying for the annual estimated volume of sediment that reaches the basin ( $59.2 \text{ km}^3 \text{ kyr}^{-1}$ ), one would get a sediment accumulation for the entire systems tract of  $106.6 \times 10^6 \text{ tons yr}^{-1}$ . This amount of sediment is partitioned roughly half in the continental realm and half offshore (Fig. 14). The offshore component (about  $53 \times 10^6 \text{ tons yr}^{-1}$ ), thus, compares with the combined sediment load from the Po plus the Apennine rivers measured today ( $47.5 \times 10^6 \text{ tons yr}^{-1}$  – Cattaneo et al., 2003; a model-calculated post-dam sediment discharge is  $43 \times 10^6 \text{ tons yr}^{-1}$  – Syvitski and Kettner, 2007). This implies that the amount of sediment that reaches the coastal

zone today is about 15% less than what could be expected before the dams were constructed in the catchments.

Sediment budget calculations, as described above, have the following implications (Fig. 14):

1. Sediment delivery per unit of time was significantly greater at lowstand times than during sea-level rise or highstand. The larger sediment volume of the LST is likely to reflect, in first approximation, the dramatic (two-fold) increase of the catchment area due to sea-level fall (Maselli et al., 2011), which was also the major driver of sediment production (Milliman and Syvitski, 1992).
2. Sediment delivery per unit of time was at its minimum under conditions of rapid sea-level rise (TST), as expected. The continental areas subject to erosion and sediment production shrank significantly in

- response to the 125-m sea-level rise, and incised valleys were backfilled, becoming sequestration areas for sediment. Nevertheless, a significant component of sediment was stored in the coastal prisms and on the continental shelf.
3. Sediment yield under highstand conditions was substantially higher than during transgression. Increased HST values relative to the TST were likely due to anthropogenic forcing, particularly over the last 2000 years (Maselli and Trincardi, 2013b; Anthony et al., 2014), and possibly to climatic forcing, especially during the Little Ice Age cold spell.
  4. Under lowstand conditions, the bulk of sediment accumulation was confined to the deepest parts of the basin, between the shelf edge (prograding wedge) and the structurally confined slope basin (ponded MTD deposits and sheet-like turbidites; Trincardi et al., 2004; Dalla Valle et al., 2013b). With the subsequent sea-level rise (TST), the bulk of sediment accumulation took place on the shelf, in the form of drowned offshore bars and, more recently, in a shore-parallel mud belt similar to that of the modern HST. During the modern sea-level highstand, sediment accumulation is focused dominantly on the alluvial/coastal plain prism and in the inner-shelf mud wedge, defining a compound delta geometry (Cattaneo et al., 2007). Very little sediment accumulated either in fluvial-channel deposits or offshore.

All sediment budget calculations were performed taking as a closure point the line connecting the tip of the Gargano Promontory, on the western side, to the island of Hvar, on the eastern side (dashed line in Fig. 14). During the deposition of each systems tract the sediment component exiting the northern and central Adriatic through this idealized line appears to increase through time, as advection processes increase their relevance. During lowstand times, mass-wasting or hyperpycnal flows were trapped topographically within the MAD slope basin, the only possible component escaping to the SE being related to hypopycnal plumes which, by definition, involve small suspended-sediment volumes. During transgression, a component of sediment transport to the SE became significant, and prodeltaic shelf muds were elongated in shore-parallel deposits reaching a volume on the order of 5 km<sup>3</sup> (Pellegrini et al., 2015); during highstand times the “leakage” of sediment to the SE became more important, as testified by the construction of the Gargano subaqueous delta with a volume of 30 km<sup>3</sup> (Cattaneo et al., 2003, 2007).

### 10.3. Human impact on sediment budgets

It has been demonstrated on a micropaleontological and paleoenvironmental basis (Piva et al., 2008c) that the late Holocene record in the Adriatic registered millennial-scale oscillations with alternating enhanced or reduced sediment flux from land in response to changes in the hydrological cycle. Humans have impacted river discharge through changes in land use and deforestation starting in Iron-Age times and then increasing during the Roman Epoch (Oldfield et al., 2003). Deforestation and land use changes, accompanied by river regulation during the Little Ice Age (LIA) represent the interval of maximum anthropic forcing and resulted in the deposition of 60 km<sup>3</sup> of modern Po delta and offshore sediment (representing about 1/3 of the HST volume in 1/10 of the time; Cattaneo et al., 2003). The relevance of this impact is even more significant when considering that this unit includes the deposit of the last Century, when dam construction resulted in sediment trapping, particularly during the post-World War II interval, thereby reducing significantly the sediment load of rivers; as an example, the decrease in sediment load from the Po river to the Northern Adriatic dropped from 17.2 to 6.4 Mt/year between 1933 to 1987 AD (Svitski and Kettner, 2007).

Delta growth occurred during two distinct phases of marked land use change and increasing regulation of the delta region, and increased dramatically about 500 years ago (Maselli and Trincardi, 2013b). Since

the beginning of the XVI Century the modern Po Delta developed as a supply-dominated system, comprising five main delta lobes; it was investigated by integrating VHR seismic profiles, recorded offshore from water depths as shallow as 5 m to the toe of the prodelta in about 30 m, with accurate historical cartography extending back several centuries and sedimentological and geo-chronological information from precisely positioned sediment cores (Correggiari et al., 2005a; Svitski et al., 2005). The use of combined historical and stratigraphic reconstructions of the modern Po Prodelta allowed volumetric calculations indicating an average sediment load of  $9.4 \times 10^6$  tons yr<sup>-1</sup> for Po di Pila and Po di Goro-Gnocca lobes; this estimate is remarkably consistent with the total sediment load of  $11.5 \times 10^6$  tons yr<sup>-1</sup> measured for most of the last century at the Pontelagoscuro gauge station at the apex of the delta plain.

## 11. Conclusions

Well constrained Quaternary depositional systems are ideal, largely untested sites where systems tract architecture and stratal relationships can be tied to specific positions on a known, and in some cases well-established, relative sea-level curve. In this context, the prominent Po Plain–Adriatic Sea area, where key stratigraphic surfaces can be traced over the entire system and confidently correlated across almost 1000 km, represents an excellent modern analog to build models of stratigraphic architecture within ancient fluvial to deep-marine successions.

This paper summarizes a body of sedimentological and stratigraphic research carried out in the last two decades on the well preserved middle-late Quaternary successions of the Po Plain and the Adriatic Sea. Facies data extracted from cores on the onshore portion of the system and seismic line interpretations from the offshore part form the building blocks of sequence-stratigraphic analysis.

Application of sequence-stratigraphic principles in a source-to-sink context highlights the combined, active role of subsidence and sea-level change in shaping stratigraphic architecture of this multi-source supplied system. Specifically, tectonics controlled the geometry of higher-rank (third-order) depositional sequences, while glacial/interglacial (100 kyr) cyclicity is shown to be the major driver of facies architecture within fourth-order sequences. Rapid basin subsidence facilitated sediment accumulation/preservation, especially during the long, though oscillatory, phases of sea-level fall and subsequent lowstands. As a result, the Po Plain–Adriatic system displays an exceptionally expanded succession of forced-regressive deposits that has no equivalent in previously published sequence-stratigraphic models.

With special reference to the last 30 kyr, the complementary onshore and offshore approach: (i) reveals the genetic and geometric relations along sequence boundaries in distinct segments of the system, including erosional lower boundaries of channel belts, interfluvial paleosols, shelf unconformities and distal (deep-marine) correlative conformities; (ii) outlines the role of coeval channel belts and incised-valley conduits in sediment delivery to the lowstand delta in the central Adriatic basin; (iii) documents a tripartite transgressive systems tract offshore, with a middle prograding unit of Younger Dryas age that is correlative at a regional scale with a prominent, laterally extensive paleosol identified onshore; (iv) suggests an increasing autogenic control on facies architecture in the highstand systems tract, due to the overwhelming effect of distributary channel avulsions, delta lobe switching and abandonment; (v) places in the proper “historical” perspective any assessment of, often unaware, human impacts on the coastal and offshore environment.

Sediment budget calculations show that sediment delivery per unit of time was significantly greater at lowstand times, when catchment areas increased dramatically due to sea-level fall, than during the subsequent phases of sea-level rise and highstand. Under lowstand conditions, the bulk of sediment accumulation was confined to the

huge LGM lowstand delta. With ensuing sea-level rise, the major loci of sediment storage shifted toward the shelf. During the modern sea-level highstand, sediment accumulation was focused dominantly on the alluvial/coastal plain prism and in the inner-shelf mud wedge. A significant perturbation by human activities over the last 500 years resulted in a >3 fold increase in the delivery of sediment to the continental shelf, before the last 50 years of pervasive dam construction.

## Acknowledgments

We are indebted to Luigi Bruno, Bruno Campo, Agnese Morelli, and Claudio Pellegrini for the fruitful discussions during preparation of this manuscript. This paper benefited from comments and constructive criticism by Janok Bhattacharya and Chuck Nittrouer. This work was partly supported by the national project RITMARE (The Italian Research for the Sea coordinated by the Italian National Research Council and funded by the Italian Ministry of Education, University and Research within the National Research Program 2011–2013). We acknowledge with gratitude the encouragement, support, and intellectual stimulation of Exxonmobil Upstream Research Company in Houston.

## References

- Abdullah, K., Anderson, J.B., Snow, J.N., Holdford-jack, L., 2004. The Late Quaternary Brazos and Colorado deltas, offshore Texas. Their evolution and the factors that controlled their deposition. In: Anderson, J.B., Fillon, R.H. (Eds.), Late Quaternary Stratigraphic Evolution of the Northern Gulf of Mexico Margin. SEPM, Special Publication 79, pp. 237–269.
- Aitken, J.F., Flint, S.S., 1996. Variable expressions of interfluvial sequence boundaries in the Breathitt Group (Pennsylvanian), eastern Kentucky, USA. In: Howell, J.A., Aitken, J.F. (Eds.), High Resolution Sequence Stratigraphy: Innovations and Applications. Spec. Publ. Geol. Soc. London 104, pp. 193–206.
- Alexander, C.R., Walsh, J.P., Orpin, A.R., 2010. Modern sediment dispersal and accumulation on the outer Poverty continental margin. Mar. Geol. 270, 213–226.
- Allen, P.A., 2008. From landscapes into the geological history. Nature 451, 274–276.
- Amorosi, A., 2012. Chromium and nickel as indicators of source-to-sink sediment transfer in a Holocene alluvial and coastal system (Po Plain, Italy). Sediment. Geol. 280, 260–269.
- Amorosi, A., Marchi, N., 1999. High-resolution sequence stratigraphy from piezocene tests: an example from the Late Quaternary deposits of the SE Po Plain. Sediment. Geol. 128, 69–83.
- Amorosi, A., Sammartino, I., 2007. Influence of sediment provenance on background values of potentially toxic metals from near-surface sediments of Po coastal plain (Italy). Int. J. Earth Sci. 96, 389–396.
- Amorosi, A., Sammartino, I., 2014. Tracing provenance and pathways of late Holocene fluvio-deltaic sediments by heavy-metal spatial distribution (Po Plain–Northern Apennines system, Italy). In: Scott, R.A., Smyth, H.R., Morton, A.C., Richardson, N. (Eds.), Sediment Provenance Studies in Hydrocarbon Exploration and Production. Geological Society Special Publication 386, pp. 313–325.
- Amorosi, A., Colalongo, M.L., Fusco, F., Pasini, G., Fiorini, F., 1999b. Glacio-eustatic control of continental-shallow marine cyclicity from Late Quaternary deposits of the south-eastern Po Plain (Northern Italy). Quat. Res. 52, 1–13.
- Amorosi, A., Colalongo, M.L., Pasini, G., Preti, D., 1999a. Sedimentary response to Late Quaternary sea-level changes in the Romagna coastal plain (northern Italy). Sedimentology 46, 99–121.
- Amorosi, A., Bruno, L., Campo, B., Morelli, A., 2015. The value of pocket penetration tests for the high-resolution palaeosol stratigraphy of late Quaternary deposits. Geol. J. 50, 670–682.
- Amorosi, A., Bruno, L., Rossi, V., Severi, P., Hajdas, I., 2014. Paleosol architecture of a late Quaternary basin-margin sequence and its implications for high-resolution, non-marine sequence stratigraphy. Glob. Planet. Chang. 112, 12–25.
- Amorosi, A., Centineo, M.C., Colalongo, M.L., Fiorini, F., 2005. Millennial-scale depositional cycles from the Holocene of the Po Plain, Italy. Mar. Geol. 222–223, 7–18.
- Amorosi, A., Centineo, M.C., Colalongo, M.L., Pasini, G., Sarti, G., Vaiani, S.C., 2003. Facies architecture and latest Pleistocene-Holocene depositional history of the Po Delta (Comacchio area) Italy. J. Geol. 111, 39–56.
- Amorosi, A., Centineo, M.C., Dinelli, E., Lucchini, F., Tateo, F., 2002. Geochemical and mineralogical variations as indicators of provenance changes in Late Quaternary deposits of SE Po Plain. Sediment. Geol. 151, 273–292.
- Amorosi, A., Colalongo, M.L., Dinelli, E., Lucchini, F., Vaiani, S.C., 2007. Cyclic variations in sediment provenance from late Pleistocene deposits of the eastern Po Plain, Italy. In: Arribas, J., Critelli, S., Johnsson, M.J. (Eds.), Sedimentary Provenance and Petrogenesis: Perspectives from Petrography and Geochemistry. Geol. Soc. of Am. Sp. Paper 420, pp. 13–24.
- Amorosi, A., Colalongo, M.L., Fiorini, F., Fusco, F., Pasini, G., Vaiani, S.C., Sarti, G., 2004. Palaeogeographic and palaeoclimatic evolution of the Po Plain from 150-ky core records. Glob. Planet. Chang. 40, 55–78.
- Amorosi, A., Dinelli, E., Rossi, V., Vaiani, S.C., Sacchetto, M., 2008a. Late Quaternary palaeoenvironmental evolution of the Adriatic coastal plain and the onset of Po River Delta. Palaeogeogr. Palaeoclimatol. Palaeoecol. 268, 80–90.
- Amorosi, A., Pavesi, M., Ricci Lucchi, M., Sarti, G., Piccin, A., 2008b. Climatic signature of cyclic fluvial architecture from the Quaternary of the central Po Plain, Italy. Sediment. Geol. 209, 58–68.
- Amorosi, A., Rossi, V., Sarti, G., Mattei, R., 2013a. Coalescent valley fills from the Late Quaternary record of Tuscany (Italy). Quatern. Int. 288, 129–138.
- Amorosi, A., Rossi, V., Vella, C., 2013b. Stepwise post-glacial transgression in the Rhône Delta area as revealed by high-resolution core data. Palaeogeogr. Palaeoclimatol. Palaeoecol. 374, 314–326.
- Anderson, J.B., Rodriguez, A., Abdulah, K.C., Fillon, R.H., Banfield, L.A., McKeown, H.A., Wllner, J.S., 2004. Late Quaternary stratigraphic evolution of the northern Gulf of Mexico Margin: a synthesis. In: Anderson, J.B., Fillon, R.H. (Eds.), Late Quaternary Stratigraphic Evolution of the Northern Gulf of Mexico Margin. SEPM, Special Publication 79, pp. 237–269.
- Anthony, E.J., Marriner, N., Morhange, C., 2014. Human influence and the changing geomorphology of Mediterranean deltas and coasts over the last 6000 years: from progradation to destruction phase? Earth Sci. Rev. 139, 336–361.
- Artegiani, A., Salusti, E., 1987. Field observations on the flow of dense water on the bottom of the Adriatic Sea during the winter 1981. Oceanol. Acta 10, 387–391.
- Artegiani, A., Bregant, D., Paschini, E., Pinardi, N., Raicich, F., Russo, A., 1997. The Adriatic sea general circulation. Part I : air-sea interactions and water mass structure. J. Phys. Oceanogr. 14, 1492–1514.
- Asioli, A., 1996. High-resolution foraminifera biostratigraphy in the central Adriatic basin during the last deglaciation: a contribution to the PALICLAS project. Mem. Ist. Ital. Idrobiol. 55, 197–217.
- Asioli, A., Trincardi, F., Lowe, J.J., Ariztegui, D., Langone, L., Oldfield, F., 2001. Sub-millennial scale climatic oscillations in the central Adriatic during the Lateglacial: paleoceanographic implications. Quat. Sci. Rev. 20, 1201–1221.
- Asioli, A., Trincardi, F., Lowe, J.J., Oldfield, F., 1999. Short-term climate changes during the last Glacial–Holocene transition: comparison between the Mediterranean and North Atlantic records. J. Quat. Sci. 4, 3732–3781.
- Bard, E., Hamelin, B., Arnold, M., Montaggioni, L., Cabioch, G., Faure, G., Rougerie, F., 1996. Deglacial sea-level record from Tahiti corals and the timing of global meltwater discharge. Nature 382, 241–244.
- Bard, E., Hamelin, B., Fairbanks, R.G., Zindler, A., 1990. Calibration of the  $^{14}\text{C}$  timescale over the past 30,000 years using mass spectrometric U-Th ages from Barbados corals. Nature 345, 405–410.
- Benetazzo, A., Bergamasco, A., Bonaldo, D., Falcieri, F.M., Sclavo, M., Langone, L., Carniel, S., 2014. Response of the Adriatic Sea to an intense cold air outbreak: dense water dynamics and wave-induced transport. Prog. Oceanogr. <http://dx.doi.org/10.1016/j.pocean.2014.08.015>.
- Bergamasco, A., Oguz, T., Malanotte-Rizzoli, P., 1999. Modeling dense water mass formation and winter circulation in the northern and central Adriatic Sea. J. Mar. Syst. 20, 279–300.
- Berné, S., Jouet, G., Bassetti, M.A., Dennielou, B., Taviani, M., 2007. Late Glacial to Preboreal sea-level rise recorded by the Rhône deltaic system (NW Mediterranean). Mar. Geol. 245, 65–88.
- Bhattacharya, J.P., 2011. Practical problems in the application of the sequence stratigraphic method and key surfaces: integrating observations from ancient fluvial–deltaic wedges with Quaternary and modelling studies. Sedimentology 58, 120–169.
- Bhattacharya, J.P., Giosan, L., 2003. Wave-influenced deltas: geomorphological implications for facies reconstruction. Sedimentology 50, 187–210.
- Bianchini, G., Laviano, R., Lovo, S., Vaccaro, C., 2002. Chemical-mineralogical characterisation of clay sediments around Ferrara (Italy): a tool for environmental analysis. Appl. Clay Sci. 21, 165–176.
- Bianchini, G., Natali, C., Di Giuseppe, D., Beccaluva, L., 2012. Heavy metals in soils and sedimentary deposits of the Padanian Plain (Ferrara, Northern Italy): characterisation and biomonitoring. J. Soils Sediments 12, 1145–1153.
- Blockley, S.P.E., Lowe, J.J., Walker, M.J.C., Asioli, A., Trincardi, F., Cope, G.R., Donahue, R.E., Pollard, A.M., 2004. Bayesian analysis of radiocarbon chronologies: examples from the European Late-glacial. J. Quat. Sci. 19, 159–175.
- Blum, M.D., Aslan, A., 2006. Signatures of climate vs. sea-level change within incised valley-fill successions: Quaternary examples from the Texas Gulf Coast. Sediment. Geol. 190, 177–211.
- Blum, M.D., Pecha, M., 2014. Mid-Cretaceous to Paleocene North American drainage reorganization from detrital zircons. Geology 42, 607–610.
- Blum, M.D., Törnqvist, T.E., 2000. Fluvial responses to climate and sea-level change: a review and look forward. Sedimentology 47, 2–48.
- Blum, M.D., Womack, J.H., 2009. Climate change, sea level change, and fluvial sediment supply to deepwater systems. In: Kneller, B., Martinsen, O.J., McCaffrey, B. (Eds.), External Controls on Deep Water Depositional Systems: Climate, Sea Level, and Sediment Flux. SEPM Special Publication 92, pp. 15–39 (Tulsa, OK).
- Blum, M.D., Martin, J., Milliken, K., Garvin, M., 2013. Paleovalley systems: Insights from Quaternary analogs and experiments. Earth-Sci. Rev. 116, 128–169.
- Blum, M.D., Tomkin, J.H., Purcell, A., Lancaster, R.R., 2008. Ups and downs of the Mississippi Delta. Geology 36, 675–678.
- Boldrin, A., Carniel, S., Giani, M., Marini, M., Bernardi Aubry, F., Campanelli, A., Grilli, F., Russo, A., 2009. Effects of bora wind on physical and biogeochemical properties of stratified waters in the northern Adriatic. J. Geophys. Res. 114, C08S92. <http://dx.doi.org/10.1029/2008JC004837>.
- Bondesan, M., Favero, V., Viñals, M.J., 1995. New evidence on the evolution of the Po Delta coastal plain during the Holocene. Quat. Int. 29–30, 105–110.
- Bourne, A.J., Lowe, J.J., Trincardi, F., Asioli, A., Blockley, S.P.E., Wulf, S., Matthews, I.P., Piva, A., Vigliotti, L., 2010. Distal tephra record for the last ca. 105,000 years from core

- PRAD1–2 in the central Adriatic Sea: implications for marine tephrostratigraphy. *Quat. Sci. Rev.* 23–24, 3079–3094.
- Boyd, R., Dalrymple, R.W., Zaitlin, B.A., 2006. Estuarine and incised-valley facies models. In: Posamentier, H.W., Walker, R.G. (Eds.), *Facies models revisited*. SEPM Special Publication 84, pp. 171–235.
- Brommer, M.B., 2009. Mass-balanced stratigraphy – data model comparison within a closed sedimentary system (Adriatic Sea, Italy) (Ph.D Thesis) University of Delft (155 pp.).
- Brommer, M.B., Weltje, G.J., Trincardi, F., 2009. Reconstruction of sediment supply from mass accumulation rates in the Northern Adriatic Basin (Italy) over the past 19,000 years. *J. Geophys. Res.* 114, F02008.
- Bruno, L., Amorosi, A., Curina, R., Severi, P., Bitelli, R., 2013. Human–landscape interactions in the Bologna area (northern Italy) during the mid-late Holocene, with focus on the Roman period. *The Holocene* 23, 1560–1571.
- Burrato, P., Ciucci, F., Valensise, G., 2003. An inventory of river anomalies in the Po Plain, Northern Italy: evidence for active blind thrust faulting. *Ann. Geophys.* 46, 865–882.
- Busschers, F.S., Kasse, C., van Balen, R.T., Vandenberghe, J., Cohen, K.M., Weerts, H.J.T., Wallinga, J., Johns, C., Cleveringa, P., Bunnik, F.P.M., 2007. Late Pleistocene evolution of the Rhine–Meuse system in the southern North Sea basin: imprints of climate change, sea-level oscillation, and glacio-isostacy. *Quat. Sci. Rev.* 26, 3216–3248.
- Calanchi, N., Cattaneo, A., Dinelli, E., Gasparotto, G., Lucchini, F., 1998. Tephra layers in Late Quaternary sediments of the central Adriatic Sea. *Mar. Geol.* 149, 191–209.
- Calvès, G., Toucanne, S., Jouet, G., Charrier, S., Thereau, E., Etoubleau, J., Marsset, T., Droz, L., Bez, M., Abreu, V., Jorry, S., Mulder, T., Lercolais, G., 2013. Inferring denudation variations from the sediment record; an example of the last glacial cycle record of the Golo Basin and watershed, East Corsica, western Mediterranean sea. *Basin Res.* 25, 197–218.
- Canals, M., Lastras, G., Urgeles, R., Casamor, J.L., Mienert, J., Cattaneo, A., De Batist, M., Haflidason, H., Imbo, Y., Laberg, J.S., Locat, J., Long, D., Longva, O., Masson, D.G., Sultan, N., Trincardi, F., Bryn, P., 2004. Slope failure dynamics and impacts from seafloor and shallow sub-seafloor geophysical data: case studies from the COSTA project. *Mar. Geol.* 213, 9–72.
- Caputo, R., Iordanidou, K., Minarelli, L., Papathanassiou, G., Poli, M.E., Rapti-Caputo, D., Sboras, S., Stefanī, M., Zanferrari, A., 2012. Geological evidence of pre-2012 seismic events, Emilia–Romagna, Italy. *Ann. Geophys.* 55, 743–749.
- Carminati, E., Vadacca, L., 2010. Two- and three-dimensional numerical simulations of the stress field at the thrust front of the Northern Apennines, Italy. *J. Geophys. Res.* 115, <http://dx.doi.org/10.1029/2010JB007870>.
- Carminati, E., Martinelli, G., Severi, P., 2003. Influence of glacial cycles and tectonics on natural subsidence in the Po Plain (northern Italy): insights from  $^{14}\text{C}$  ages. *G3* 4, <http://dx.doi.org/10.1029/2002GC000481>.
- Carniel, S., Trincardi, F., Bonaldo, D., Benetazzo, A., Bergamasco, A., Boldrin, A., Falcieri, F.M., Langone, L., Scavo, M., 2015. Off-shelf fluxes across the southern Adriatic margin: factors controlling dense-water-driven transport phenomena. *Mar. Geol.* <http://dx.doi.org/10.1016/j.margeo.2015.08.016>.
- Carter, L., Orpin, A.R., Kuehl, S.A., 2010. From mountain source to ocean sink – the passage of sediment across an active margin, Waipaoa Sedimentary System, New Zealand. *Mar. Geol.* 270, 1–10.
- Castiglioni, G.B., Biancotti, A., Bondesan, M., Cortemiglia, G.C., Elmi, C., Favero, V., Gasperi, G., Marchetti, G., Orombelli, G., Pellegrini, G.B., Tellini, C., 1999. Geomorphological map of the Po Plain, Italy, at a scale of 1:250,000. *Earth Surf. Process. Landf.* 24, 1115–1120.
- Cattaneo, A., Steel, R.J., 2003. Transgressive deposits: a review of their variability. *Earth Sci. Rev.* 62, 187–228.
- Cattaneo, A., Trincardi, F., 1999. The Late Quaternary transgressive record in the Adriatic epicontinent sea: basin widening and facies partitioning. In: Bergman, K.M., Snedden, J.W. (Eds.), *Isolated Shallow Marine Sand Bodies: Sequence Stratigraphic Analysis and Sedimentological Interpretation*. SEPM Special Publication 64, pp. 127–146.
- Cattaneo, A., Correggiari, A., Langone, L., Trincardi, F., 2003. The Late-Holocene Gargano subaqueous delta, Adriatic shelf: sediment pathways and supply fluctuations. *Mar. Geol.* 193, 61–91.
- Cattaneo, A., Correggiari, A., Marsset, T., Thomas, Y., Marsset, B., Trincardi, F., 2004. Seafloor undulation pattern on the Adriatic shelf and comparison to deep-water sediment waves. *Mar. Geol.* 213, 121–148.
- Cattaneo, A., Trincardi, F., Asioli, A., Correggiari, A., 2007. The Western Adriatic shelf clineform: energy-limited bottomset. *Cont. Shelf Res.* 27, 506–525.
- Catuneanu, O., Abreu, V., Bhattacharya, J.P., Blum, M.D., Dalrymple, R.W., Eriksson, P.G., Fielding, C.R., Fisher, W.L., Galloway, W.E., Gibling, M.R., Giles, K.A., Holbrook, J.M., Jordan, R., Kendall, C.G.S.C., Macurda, B., Martinsen, O.J., Miall, A.D., Neal, J.E., Nummedal, D., Pomar, L., Posamentier, H.W., Pratt, B.R., Sarg, J.F., Shanley, K.W., Steel, R.J., Strasser, A., Tucker, M.E., Winker, C., 2009. Towards the standardization of sequence stratigraphy. *Earth Sci. Rev.* 92, 1–33.
- Chappell, J., Shackleton, N.J., 1986. Oxygen isotopes and sea level. *Nature* 324, 137–140.
- Chiggiano, J., Bergamasco, A., Borghini, M., Falcieri, F.M., Falco, P., Langone, L., Misericochi, S., Russo, A., Schroeder, K., 2015. Dense-water bottom currents in the Southern Adriatic Sea in spring 2012. *Mar. Geol.* <http://dx.doi.org/10.1016/j.margeo.2015.09.005>.
- Ciabatti, M., 1967. Ricerche sull'evoluzione del Delta Padano. *Giorn. Geol.* 34, 381–406.
- Ciabatti, M., Curzi, P.V., Ricci Lucchi, F., 1987. Quaternary sedimentation in the Central Adriatic Sea. *Giorn. Geol.* 49, 113–125.
- Cleveland, D.M., Atchley, S.C., Nordt, L.C., 2007. Continental sequence stratigraphy of the Upper Triassic (Norian–Rhaetian) Chinle Strata, Northern New Mexico, U.S.A.: allocyclic and autocyclic origins of paleosol-bearing alluvial successions. *J. Sediment. Res.* 77, 909–924.
- Correggiari, A., Field, M.E., Trincardi, F., 1996b. Late Quaternary transgressive large dunes on the sediment-starved Adriatic shelf. In: De Batist, M., Jacobs, P. (Eds.), *Geology of Siliciclastic Shelf Seas*. Geological Society Special Publication 117, pp. 155–169.
- Correggiari, A., Roveri, M., Trincardi, F., 1996a. Late Pleistocene and Holocene evolution of the north Adriatic Sea. *Il Quaternario* 9, 697–704.
- Correggiari, A., Cattaneo, A., Trincardi, F., 2005a. Depositional patterns in the late Holocene Po delta system. In: Giosan, L., Bhattacharya, P. (Eds.), *River Deltas – Concepts, Models, and Examples*. SEPM Special Publication 83, pp. 365–392.
- Correggiari, A., Cattaneo, A., Trincardi, F., 2005b. The modern Po Delta system: lobe switching and asymmetric prodelta growth. *Mar. Geol.* 222–223, 49–74.
- Covault, J.A., Romans, B.W., Graham, S.A., Fildani, A., Hilley, G.E., 2011. Terrestrial source to deep-sea sink sediment budgets at high and low sea levels: Insights from tectonically active Southern California. *Geology* 39, 619–622.
- Curzi, P.V., Dinelli, E., Ricci, L.M., Vaiani, S.C., 2006. Palaeoenvironmental control on sediment composition and provenance in the late Quaternary deltaic successions: a case study from the Po delta area (Northern Italy). *Geol. J.* 41, 591–612.
- Dabrio, C.J., Zazo, C., Goy, J.L., Sierra, F.J., Borja, F., Lario, J., González, J.A., Flores, J.A., 2000. Depositional history of estuarine infill during the last postglacial transgression (Gulf of Cadiz, Southern Spain). *Mar. Geol.* 162, 381–404.
- Dalla Valle, G., Gamberi, F., Rocchini, P., Minisini, D., Errera, A., Baglioni, L., Trincardi, F., 2013b. 3D seismic geomorphology of mass transport complexes in a foredeep basin: examples from the Pleistocene of the Central Adriatic Basin (Mediterranean Sea). *Sediment. Geol.* 294, 126–141.
- Dalla Valle, G., Gamberi, F., Trincardi, F., Rocchini, P., Errera, A., Baglioni, L., 2013a. Contrasting slope channel styles on a prograding mud-prone margin. *Mar. Pet. Geol.* 41, 72–82.
- Dalrymple, R.W., Boyd, R., Zaitlin, B.A., 1994. Incised-valley systems: origin and sedimentary sequences. *SEPM Spec. Publ.* 51 (391 pp.).
- Dinelli, E., Ghosh, A., Rossi, V., Vaiani, S.C., 2013. Multiproxy reconstruction of Late Pleistocene–Holocene environmental changes in coastal successions: microfossil and geochemical evidences from the Po Plain (Northern Italy). *Stratigraphy* 9, 153–167.
- Doglioni, C., 1993. Some remarks on the origin of foredeeps. *Tectonophysics* 228, 1–20.
- Doglioni, C., Mongelli, F., Pieri, P., 1994. The Puglia uplift (SE Italy): an anomaly in the foreland of the Apennine subduction due to buckling of a thick continental lithosphere. *Tectonics* 13, 1309–1321.
- Donnici, S., Serandrei-Barbero, R., Bini, C., Bonardi, M., Lezziero, A., 2011. The caranto paleosol and its role in the early urbanization of Venice. *Geoarchaeology* 26, 514–543.
- Fairbanks, R.G., 1989. A 17,000-year glacio-eustatic sea level record: influence of glacial melting rates on the Younger Dryas event and deep-ocean circulation. *Nature* 342, 637–642.
- Falcieri, F.M., Benetazzo, A., Scavo, M., Russo, A., Carniel, S., 2013. Po River plume pattern variability investigated from model data. *Cont. Shelf Res.* <http://dx.doi.org/10.1016/j.csr.2013.11.001>.
- Ferranti, L., Antonioli, F., Mauz, B., Amorosi, A., Dai, P.G., Mastronuzzi, G., Monaco, C., Orrù, P., Pappalardo, M., Radtke, U., Renda, P., Romano, P., Sansò, P., Verrubbi, V., 2006. Markers of the last interglacial sea-level high stand along the coast of Italy: tectonic implications. *Quat. Int.* 145–146, 30–54.
- Follieri, M., Magri, D., Sadoni, L., 1988. 250,000-year pollen record from Valle di Castiglione (Roma). *Pollen Spores* 30, 329–356.
- Fontana, A., Mozzi, P., Bondesan, A., 2008. Alluvial megafans in the Venetian–Friulian Plain (north-eastern Italy): evidence of sedimentary and erosive phases during Late Pleistocene and Holocene. *Quat. Int.* 189, 71–90.
- Frignani, M., Langone, L., Ravaioli, M., Sorgente, D., Alvisi, F., Albertazzi, S., 2005. Fine-sediment mass balance in the western Adriatic continental shelf over a century time scale. *Mar. Geol.* 222–223, 113–133.
- Galloway, W.E., 1975. Process framework for describing the morphologic and stratigraphic evolution of deltaic depositional systems. In: Broussard, M.L. (Ed.), *Deltas, Models for Exploration*. Houston Geological Society, pp. 87–98 (Houston, TX).
- Gerber, T.P., Pratson, L.F., Kuhel, S., Walsh, J.P., Alexander, C., Palmer, A., 2010. The influence of sea level and tectonics on Late Pleistocene through Holocene sediment storage along the high-sediment supply Waipaoa continental shelf. *Mar. Geol.* 270, 139–159.
- Ghielmi, M., Minervini, M., Nini, C., Rogledi, S., Rossi, M., 2013. Late Miocene–Middle Pleistocene sequences in the Po Plain–Northern Adriatic Sea (Italy): the stratigraphic record of modification phases affecting a complex foreland basin. *Mar. Pet. Geol.* 42, 50–81.
- Gibling, M.R., Bird, D.J., 1994. Late Carboniferous cyclothsems and alluvial paleovalleys in the Sydney basin, Nova Scotia. *Geol. Soc. Am. Bull.* 106, 105–117.
- Gibling, M.R., Wightman, W.G., 1994. Paleovalleys And Protozoan assemblages in a Late Carboniferous cyclothem, Sydney Basin, Nova Scotia. *Sedimentology* 41, 699–719.
- Gibling, M.R., Fielding, C.R., Sinha, R., 2011. Alluvial valleys and alluvial sequences: towards a geomorphic assessment. In: Davidson, S.K., Leleu, S., North, C.P. (Eds.), *From River to Rock Record: The Preservation of Fluvial Sediments and their Subsequent Interpretation*. SEPM Society for Sedimentary Geology Special Publication 97, pp. 423–447.
- Guillocheau, F., Rouby, D., Robin, C., Helm, C., Rolland, N., Le Carlier de Veslud, C., Braun, J., 2011. Quantification and causes of the terrigenous sediment budget at the scale of a continental margin: a new method applied to the Namibia–South Africa margin. *Basin Res.* 24, 3–30.
- Hanneman, D.L., Wideman, C.J., 2006. Sequence stratigraphy of Cenozoic continental rocks. *Geol. Soc. Am. Bull.* 103, 1335–1345.
- Hays, J.D., Imbrie, J., Shackleton, N.J., 1976. Variations in the earth's orbit: pacemaker of the ice ages. *Science* 194, 1121–1132.
- Hernández-Molina, F.J., Somoza, L., Rey, J., Pomar, L., 1994. Late Pleistocene–Holocene sediments on the Spanish continental shelves: model for very high resolution sequence stratigraphy. *Mar. Geol.* 120, 129–174.
- Holbrook, J., Wanás, H., 2014. A fulcrum approach to assessing source-to-sink mass balance using channel paleohydrologic parameters derivable from common fluvial data sets with an example from the Cretaceous of Egypt. *J. Sediment. Res.* 84, 349–372.
- Hunt, D., Tucker, M.E., 1992. Stranded parasequences and the forced regressive wedge systems tract: deposition during base-level fall. *Sediment. Geol.* 81, 1–9.

- Kasse, C., Bohncke, S.J.P., Vandenberghe, J., Gábris, G., 2010. Fluvial style changes during the last glacial–interglacial transition in the middle Tisza valley (Hungary). *Proc. Geol. Assoc.* 121, 180–194.
- Kettner, A.J., Syvitski, J.P.M., 2008. Predicting discharge and sediment flux of the Po River, Italy since the Last Glacial Maximum. In: de Boer, P., Postma, G., van der Zwan, K., Burgess, P., Kukla, P. (Eds.), *Analogue and Numerical Modelling of Sedimentary Systems: From Understanding to Prediction*. Wiley-Blackwell, Oxford, UK.
- Kowalewski, M., Wittmer, J.M., Dexter, T.A., Amorosi, A., Scarponi, D., 2015. Differential response of marine communities to natural and anthropogenic changes. *Proc. R. Soc. B* 282. <http://dx.doi.org/10.1098/rspb.2014.2990>.
- Lauer, W.J., Parker, G., Dietrich, W.E., 2008. Response of Strickland and Fly River confluence to postglacial sea level rise. *J. Geophys. Res.* 113. <http://dx.doi.org/10.1029/2006JF000626>.
- Listecki, L.E., Raymo, M.E., 2005. A Pliocene-Pleistocene stack of 57 globally distributed benthic  $\delta^{18}\text{O}$  records. *Paleoceanography* 20, PA1003. <http://dx.doi.org/10.1029/2004PA001071>.
- Lobo, F.J., Ridente, D., 2014. Stratigraphic architecture and spatio-temporal variability of high-frequency (Milankovitch) depositional cycles on modern continental margins: an overview. *Mar. Geol.* 352, 215–247.
- Lowe, J.J., Blockley, S., Trincardi, F., Asioli, A., Cattaneo, A., Matthews, I.P., Pollard, M., Wulf, S., 2007. Age modelling of late Quaternary marine sequences in the Adriatic: towards improved precision and accuracy using volcanic event stratigraphy. *Cont. Shelf Res.* 27, 560–582.
- Mack, G.H., Tabor, N.J., Zollinger, H.J., 2010. Palaeosols and sequence stratigraphy of the Lower Permian Abo Member, south-central New Mexico, USA. *Sedimentology* 57, 1566–1583.
- Marchesini, L., Amorosi, A., Cibin, U., Zuffa, G.G., Spadafora, E., Preti, D., 2000. Sand composition and sedimentary evolution of a Late Quaternary depositional sequence, north-western Adriatic Coast, Italy. *J. Sediment. Res.* 70, 829–838.
- Marini, M., Maselli, V., Campanelli, A., Foglini, F., Grilli, F., 2015. Role of the Mid-Adriatic deep in dense water interception and modification. *Mar. Geol.* <http://dx.doi.org/10.1016/j.margeo.2015.08.015>.
- Martinsen, O.J., Sømme, T.O., Thurmond, J.B., Helland-Hansen, W., Lunt, I., 2010. Source-to-sink systems on passive margins: theory and practice with an example from the Norwegian continental margin. In: Vining, B.A., Pickering, S.C. (Eds.), *Petroleum Geology: From Mature Basins to New Frontiers – Proceedings of the 7th Petroleum Geology Conference*. Geological Society, London, pp. 913–920.
- Maselli, V., Trincardi, F., 2013a. Large-scale single incised valley from a small catchment basin on the western Adriatic margin (central Mediterranean Sea). *Glob. Planet. Chang.* 100, 245–262.
- Maselli, V., Trincardi, F., 2013b. Man made deltas. *Sci. Rep.* 3. <http://dx.doi.org/10.1038/srep01926>.
- Maselli, V., Hutton, E.W., Kettner, A.J., Syvitski, J.P.M., Trincardi, F., 2011. High-frequency sea level and sediment supply fluctuations during Termination I: an integrated sequence-stratigraphy and modeling approach from the Adriatic Sea (Central Mediterranean). *Mar. Geol.* 287, 54–70.
- Maselli, V., Trincardi, F., Asioli, A., Ceregato, A., Rizzetto, F., Taviani, M., 2014. Delta growth and river valleys: the influence of climate and sea level changes on the South Adriatic shelf (Mediterranean Sea). *Quat. Sci. Rev.* 99, 146–163.
- Maselli, V., Trincardi, F., Cattaneo, A., Ridente, D., Asioli, A., 2010. Subsidence pattern in the central Adriatic and its influence on sediment architecture during the last 400 kyr. *J. Geophys. Res.* 115, B12106. <http://dx.doi.org/10.1029/2010JB007687>.
- McCarthy, P.J., Plint, A.G., 1998. Recognition of interfluvial sequence boundaries: integrating paleopedology and sequence stratigraphy. *Geology* 26, 387–390.
- Milliman, J.D., Syvitski, J.P.M., 1992. Geomorphic/tectonic control of sediment discharge to the ocean: the importance of small mountainous rivers. *J. Geol.* 100, 525–544.
- Mitchum Jr., R.M., Vail, P.R., Thompson III, S., 1977. The depositional sequence as a basic unit for stratigraphic analysis. In: Payton, C.E. (Ed.), *Seismic Stratigraphy – Application for Hydrocarbon Exploration*. American Association of Petroleum Geologists Memoir 26, pp. 53–62.
- Muttoni, G., Carcano, C., Garzanti, E., Ghielmi, M., Piccin, A., Pini, R., Rogledi, S., Sciunnach, D., 2003. Onset of major Pleistocene glaciations in the Alps. *Geology* 31, 989–992.
- Nelson, B.W., 1970. Hydrography, sediment dispersal, and recent historical development of the Po River delta, Italy. *SEPM Spec. Publ.* 15, 152–184.
- Nittrouer, C.A., Miserocchi, S., Trincardi, F., 2004. The PASTA Project: investigation of the Po and apennine sediment transport and accumulation. *Oceanography* 17, 46–57.
- Oldfield, F., Asioli, A., Accorsi, C.A., Mercuri, A.M., Juggins, S., Langone, L., Rolph, T., Trincardi, F., Wolff, G., Gibbs, Z., Vigliotti, L., Frignani, M., van der Post, K., Branch, N., 2003. A high resolution late Holocene palaeo environmental record from the central Adriatic Sea. *Quat. Sci. Rev.* 22, 319–342.
- Olsen, T., Steel, R., Hogseth, K., Skar, T., Roe, S.-L., 1995. Sequential architecture in a fluvial succession: sequence stratigraphy in the Upper Cretaceous Mesaverde Group, Price Canyon, Utah. *J. Sediment. Res.* B65, 265–280.
- Ori, G.G., 1993. Continental depositional systems of the Quaternary of the Po Plain (northern Italy). *Sediment. Geol.* 83, 1–14.
- Ori, G.G., Roveri, M., Vannoni, F., 1986. Plio-Pleistocene sedimentation in the Apenninic-Adriatic foredeep (Central Adriatic Sea, Italy). In: Allen, P.A., Homewood, P. (Eds.), *Foreland Basins*. Spec. Publ. Int. Assoc. Sediment. 8, pp. 183–198.
- Palinkas, C.M., Nittrouer, C.A., Wheatcroft, R.A., Langone, L., 2005. The use of  $7\text{Be}$  to identify event and seasonal sedimentation near the Po River delta, Adriatic Sea. *Mar. Geol.* 222–223, 95–112.
- Paola, C., Leeder, M., 2011. Environmental dynamics: simplicity versus complexity. *Nature* 469, 38–39.
- Pellegrini, C., Maselli, V., Cattaneo, A., Piva, A., Ceregato, A., Trincardi, F., 2015. Anatomy of a compound delta from the post-glacial transgressive record in the Adriatic Sea. *Mar. Geol.* 362, 43–59.
- Picotti, V., Pazzaglia, F.J., 2008. A new active tectonic model for the construction of the Northern Apennines mountain front near Bologna (Italy). *J. Geophys. Res.* 113, B08412. <http://dx.doi.org/10.1029/2007JB005307>.
- Pieri, M., Groppi, G., 1981. Subsurface geological structure of the Po Plain, Italy. *P.F. Geodin. Publ.* 414. CN.R., Roma, pp. 1–23.
- Piva, A., Asioli, A., Andersen, N., Grimalt, J.O., Schneider, R.R., Trincardi, F., 2008b. Climatic cycles as expressed in sediments of the PROMESS1 borehole PRAD1–2, central Adriatic, for the last 370 ka: 2. Paleoenvironmental evolution. *Geochem. Geophys. Geosyst.* 9, Q03R02.
- Piva, A., Asioli, A., Schneider, R.R., Trincardi, F., Andersen, N., Colmenero-Hidalgo, E., Dennielou, B., Flores, J.-A., Vigliotti, L., 2008a. Climatic cycles as expressed in sediments of the PROMESS1 borehole PRAD1–2, central Adriatic, for the last 370 ka: 1. Integrated stratigraphy. *Geochem. Geophys. Geosyst.* 9, Q01R01.
- Piva, A., Asioli, A., Trincardi, F., Schneider, R.R., Vigliotti, L., 2008c. Late-holocene climate variability in the Adriatic Sea (Central Mediterranean). *The Holocene* 18, 153–167.
- Plint, A.G., Nummedal, D., 2000. The falling stage systems tract: recognition and importance in sequence stratigraphic analysis. In: Gawthorpe, R.L., Hunt, D. (Eds.), *Sedimentary Responses to Forced Regressions*. Spec. Publ. Geol. Soc. London 172, pp. 1–17.
- Plint, A.G., McCarthy, P.J., Faccini, U.F., 2001. Nonmarine sequence stratigraphy: updip expression of sequence boundaries and systems tracts in a high-resolution framework, Cenomanian Dunvegan Formation, Alberta foreland basin, Canada. *Am. Assoc. Pet. Geol. Bull.* 85, 1967–2001.
- Posamentier, H.W., Allen, G.P., 1999. Siliciclastic sequence stratigraphy: concepts and applications. *SEPM Concepts in Sedimentology and Paleontology* 7. Society for Sedimentary Geology (204 pp.).
- Posamentier, H.W., Vail, P.R., 1988. Eustatic controls on clastic deposition II – sequence and systems tract models. In: Wilgus, C.K., Hastings, B.S., Kendall, C.G.S.C., Posamentier, H.W., Ross, C.A., Van Wagoner, J.C. (Eds.), *Sea Level Changes: An Integrated Approach*. Spec. Publ. Soc. Econ. Paleont. Miner. 42, pp. 125–154.
- Posamentier, H.W., Jersey, M.T., Vail, P.R., 1988. Eustatic controls on clastic deposition I: conceptual framework. In: Wilgus, C.K., Hastings, B.S., Kendall, C.G.S.C., Posamentier, H.W., Ross, C.A., Van Wagoner, J.C. (Eds.), *Sea Level Changes: An Integrated Approach*. Spec. Publ. Soc. Econ. Paleont. Miner. 42, pp. 109–124.
- Puig, P., Ogston, A.S., Guillén, J., Fain, A.M.V., Palanques, A., 2007. Sediment transport processes from the topset to the foreset of a crenulated clinoform (Adriatic Sea). *Cont. Shelf Res.* 27, 452–474.
- Querin, S., Cossarini, G., Solidoro, C., 2013. Simulating the formation and fate of dense water in a midlatitude marginal sea during normal and warm winter conditions. *J. Geophys. Res.* 118, 885–900.
- Regione Emilia-Romagna, ENI-AGIP, 1998. In: Di Dio, G. (Ed.), *Riserve Idriche Sotterranee Della Regione Emilia-Romagna. S.ELCA*, Firenze (120 pp.).
- Regione Lombardia, Eni Divisione Agip, 2002. In: Carcano, C., Piccin, A. (Eds.), *Geologia Degli Acquiferi Padani della Regione Lombardia. S.ELCA*, Firenze (130 pp.).
- Ricci Lucchi, F., Colalongo, M.L., Cremonini, G., Gasperi, G., Iaccarino, S., Papani, G., Raffi, S., Rio, D., 1982. Evoluzione sedimentaria e paleogeografia nel margine appenninico. In: Cremonini, G., Ricci Lucchi, F. (Eds.), *Guida Alla Geologia Del Margine Appenninico-Padano. Guida Geologica Regionale della Società Geologica Italiana*, pp. 17–46.
- Ridente, D., Trincardi, F., 2002. Eustatic and tectonic control on deposition and lateral variability of Quaternary regressive sequences in the Adriatic basin (Italy). *Mar. Geol.* 184, 273–293.
- Ridente, D., Trincardi, F., 2005. Pleistocene “muddy” forced-regression deposits on the Adriatic shelf: a comparison with prodelta deposits of the late Holocene highstand mud wedge. *Mar. Geol.* 222–223, 213–233.
- Ridente, D., Trincardi, F., 2006. Active foreland deformation evidenced by shallow folds and faults affecting late Quaternary shelf-slope deposits (Adriatic Sea, Italy). *Basin Res.* 18, 171–188.
- Ridente, D., Trincardi, F., Piva, A., Asioli, A., 2009. The combined effect of sea level and supply during Milankovitch cyclicity: evidence from shallow-marine  $\delta^{18}\text{O}$  records and sequence architecture (Adriatic margin). *Geology* 37, 1003–1006.
- Ridente, D., Trincardi, F., Piva, A., Asioli, A., Cattaneo, A., 2008. Sedimentary response to climate and sea level changes during the past 400 ka from borehole PRAD1.2 (Adriatic margin). *Geochem. Geophys. Geosyst.* 9, Q09R04.
- Rizzini, A., 1974. Holocene sedimentary cycle and heavy mineral distribution, Romagna-Marche coastal plain, Italy. *Sediment. Geol.* 11, 17–37.
- Romans, B.W., Normark, W.R., McGann, M.M., Covault, J.A., Graham, S.A., 2009. Coarse-grained sediment delivery and distribution in the Holocene Santa Monica Basin, California: implications for evaluating source-to-sink flux at millennial timescales. *Geol. Soc. Am. Bull.* 121, 1394–1408.
- Rossi, V., Horton, B.P., 2009. The application of a subtidal foraminifera-based transfer function to reconstruct Holocene paleobathymetry of the Po Delta, Northern Adriatic Sea. *J. Foraminiferal Res.* 39, 180–190.
- Rossi, V., Vaiani, S.C., 2008. Benthic foraminiferal evidence of sediment supply changes and fluvial drainage reorganization in Holocene deposits of the Po Delta. *Mar. Micropaleontol.* 69, 106–118.
- Royden, L.E., Patacca, E., Scandone, P., 1987. Segmentation and configuration of subducted lithosphere in Italy: an important control on thrust-belt and foredeep-basin evolution. *Geology* 15, 714–717.
- Saito, Y., 1994. Shelf sequence and characteristic bounding surfaces in a wave-dominated setting: Latest Pleistocene-Holocene examples from Northeast Japan. *Mar. Geol.* 120, 105–127.
- Scarponi, D., Kowalewski, M., 2004. Stratigraphic paleoecology: bathymetric signatures and sequence overprint of mollusk associations from upper Quaternary sequences of the Po Plain, Italy. *Geology* 32, 989–992.
- Scarponi, D., Kowalewski, M., 2007. Sequence stratigraphic anatomy of diversity patterns: late Quaternary benthic molluscs of the Po Plain, Italy. *Palaios* 22, 296–305.

- Scarpioni, D., Kaufman, D., Amorosi, A., Kowalewski, M., 2013. Sequence stratigraphy and the resolution of the fossil record. *Geology* 41, 239–242.
- Scrocca, D., 2006. Thrust front segmentation induced by differential slab retreat in the Apennines (Italy). *Terra Nova* 18, 154–161.
- Sgavetti, M., Ferrari, C., 1988. The use of TM data for the study of a modern deltaic depositional system. *Int. J. Remote Sens.* 9, 1613–1627.
- Shanley, K.W., McCabe, P.J., 1994. Perspectives on the sequence stratigraphy of continental strata. *Am. Assoc. Pet. Geol. Bull.* 78, 544–568.
- Sherwood, C.R., Carniel, S., Cavalieri, L., Chiggiato, J., Das, H., Doyle, J.D., Harris, C.K., Niedoroda, A.W., Pullen, J., Reed, C.W., Russo, A., Sclavo, M., Signell, R.P., Traykovski, P., Warner, J.C., 2004. Sediment dynamics in the Adriatic Sea investigated with coupled models. *Oceanography* 17, 58–69.
- Simms, A.R., Rodriguez, A.B., 2014. Where do coastlines stabilize following rapid retreat? *Geophys. Res. Lett.* 41, 1698–1703.
- Slingerland, R., Driscoll, N.W., Milliman, J.D., Miller, S.R., Johnstone, E.A., 2008. *J. Geophys. Res.* 113, F01S13.
- Soil Survey Staff, 1999. Soil taxonomy. A basic system of soil classification for making and interpreting soil surveys. 2nd edition Agricultural Handbook 436. Natural Resources Conservation Service, USDA, Washington DC, USA.
- Sømme, T.O., Jackson, C.A.-L., 2013. Source-to-sink analysis of ancient sedimentary systems using a subsurface case study from the Møre-Trøndelag area of southern Norway: part 2 – Sediment dispersal and forcing mechanisms. *Basin Res.* 25, 512–531.
- Sømme, T.O., Helland-Hansen, W., Martinsen, O.J., Thurmond, J.B., 2009. Relationships between morphological and sedimentological parameters in source-to-sink systems: a basis for predicting semi-quantitative characteristics in subsurface systems. *Basin Res.* 21, 361–387.
- Sømme, T.O., Piper, D.J.W., Deptuck, M.E., Helland-Hansen, W., 2011. Linking onshore-offshore sediment dispersal in the Golo source-to-sink system (Corsica, France) during the Late Quaternary. *J. Sediment. Res.* 81, 118–137.
- Steckler, M.S., Mountain, G.S., Miller, K.G., Christie-Blick, N., 1999. Reconstruction of Tertiary progradation and clinoform development on the New Jersey passive margin by 2-D backstripping. *Mar. Geol.* 154, 399–420.
- Stefani, M., Vincenzi, S., 2005. The interplay of eustasy, climate and human activity in the late Quaternary depositional evolution and sedimentary architecture of the Po Delta system. *Mar. Geol.* 222–223, 19–48.
- Storms, J.E.A., Weltje, G.J., Terra, G.J., Cattaneo, A., Trincardi, A., 2008. Coastal dynamics under conditions of rapid sea-level rise: Late Pleistocene to Early Holocene evolution of barrier-lagoon systems on the northern Adriatic shelf (Italy). *Quat. Sci. Rev.* 27, 1107–1123.
- Sultan, N., Cattaneo, A., Urgeles, R., Lee, H., Locat, J., Trincardi, F., Berné, S., Canals, M., Lafuerza, S., 2008. A geomechanical approach for the genesis of sediment undulations on the Adriatic shelf. *Geochim. Geophys. Geosyst.* 9, 1–25.
- Supić, N., Orlić, M., 1999. Seasonal and interannual variability of the northern Adriatic surface fluxes. *J. Mar. Syst.* 20, 205–229.
- Swenson, J.B., Paola, C., Pratson, L., Voller, V.R., Murray, A.B., 2005. Fluvial and marine controls on combined subaerial and subaqueous delta progradation: morphodynamic modeling of compound-clinoform development. *J. Geophys. Res.* 110, F02013.
- Syvitski, J.P.M., Kettner, A.J., 2007. On the flux of water and sediment into the Northern Adriatic Sea. *Cont. Shelf Res.* 27, 296–308.
- Syvitski, J.P.M., Milliman, J.D., 2007. Geology, geography, and humans battle for dominance over the delivery of fluvial sediment to the coastal ocean. *J. Geol.* 115, 1–19.
- Syvitski, J.P.M., Kettner, A.J., Correggiari, A., Nelson, B.W., 2005. Distributary channels and their impact on sediment dispersal. *Mar. Geol.* 222–223, 75–94.
- Taviani, M., Angeletti, L., Campiani, E., Ceregato, A., Foglini, F., Maselli, V., Morsilli, M., Parise, M., Trincardi, F., 2012. Drowned karst landscape offshore the Apulian margin (southern Adriatic Sea, Italy). *J. Cave Karst Stud.* 74, 197–212.
- Taviani, M., Franchi, F., Angeletti, L., Correggiari, A., López-Correa, M., Maselli, V., Mazzoli, C., Peckmann, J., 2015. Bi detrital carbonates on the Adriatic continental shelf imprinted by oxidation of sleeping hydrocarbons. *Mar. Pet. Geol.* <http://dx.doi.org/10.1016/j.marpgeo.2015.03.015>.
- Trincardi, F., Correggiari, A., 2000. Quaternary forced regression deposits in the Adriatic basin and the record of composite sea-level cycles. In: Hunt, D., Gawthorpe, R.L. (Eds.), *Sedimentary Response of Forced Regressions*. Geological Society of London, Special Publication 172, pp. 245–269.
- Trincardi, F., Foglini, F., Verdicchio, G., Asioli, A., Correggiari, A., Minisini, D., 2007a. The impact of cascading currents on the Bari Canyon System, SW-Adriatic Margin (Central Mediterranean). *Mar. Geol.* 246, 208–230.
- Trincardi, F., Verdicchio, G., Misericchi, S., 2007b. Seafloor evidence for the interaction between cascading and along-slope bottom water masses. *J. Geophys. Res.* 112, F03011.
- Trincardi, F., Campiani, E., Correggiari, A., Foglini, F., Maselli, V., Remia, A., 2014. Bathymetry of the Adriatic Sea: the legacy of the last eustatic cycle and the impact of modern sediment dispersals. *J. Maps* <http://dx.doi.org/10.1080/17445647.2013.864844>.
- Trincardi, F., Cattaneo, A., Asioli, A., Correggiari, A., Langone, L., 1996. Stratigraphy of the Late-Quaternary deposits in the central Adriatic basin and the record of short term climatic events. *Mem. Ist. Ital. Idrobiol.* 55, 39–70.
- Trincardi, F., Cattaneo, A., Correggiari, A., Ridente, D., 2004. Evidence of soft-sediment deformation, fluid escape, sediment failure and regional weak layers within the late-Quaternary mud deposits of the Adriatic Sea. *Mar. Geol.* 213, 91–119.
- Trincardi, F., Correggiari, A., Roveri, M., 1994. Late Quaternary transgressive record and deposition in a modern epicontinental shelf: the Adriatic semi-enclosed basin. *Geo-Mar. Lett.* 14, 41–51.
- Tzedakis, P.C., Andrieu, V., de Beaulieu, J.-L., Crowhurst, S., Follieri, M., Hooghiemstra, H., Magri, D., Reille, M., Sadoni, L., Shackleton, N.J., Wijmstra, T.A., 1997. Comparison of terrestrial and marine records of changing climate of the last 500,000 years. *Earth Planet. Sci. Lett.* 150, 171–176.
- Van Waggoner, J.C., Mitchum, R.M., Campion, K.M., Rahamanian, V.D., 1990. Siliciclastic sequence stratigraphy in well logs, cores and outcrops: concepts for high resolution correlations of time and facies. *American Association of American Petroleum Geologists Methods in Exploration* 7. Barbara H. Litz, Tulsa, U.S.A.
- Varela, A.N., Veiga, G.D., Poiré, D.G., 2012. Sequence stratigraphic analysis of Cenomanian greenhouse palaeosols: a case study from southern Patagonia, Argentina. *Sediment. Geol.* 271–272, 67–82.
- Veggiani, A., 1974. Le variazioni idrografiche del basso corso del fiume Po negli ultimi 3000 anni. *Padusa* 1–2, 39–60.
- Verdicchio, G., Trincardi, F., 2006. Short-distance variability in slope bed-forms along the Southwestern Adriatic Margin (Central Mediterranean). *Mar. Geol.* 234, 271–292.
- Vigliotti, L., Verosub, K.L., Cattaneo, A., Trincardi, F., Asioli, A., Piva, A., 2008. Palaeomagnetic and rock magnetic analysis of Holocene deposits from the Adriatic Sea: detecting and dating short-term fluctuations in sediment supply. *The Holocene* 18, 141–152.
- Vilibić, I., 2003. An analysis of dense water production on the North Adriatic shelf. *Estuar. Coast. Shelf Sci.* 56, 697–707.
- Vilibić, I., Supić, N., 2005. Dense water generation on a shelf: the case of the Adriatic Sea. *Ocean Dyn.* 55, 403–415.
- Waelbroeck, C., Labeyrie, L., Michel, E., Duplessy, J.C., McManus, J.F., Lambeck, K., Balbon, E., Labracherie, M., 2002. Sea-level and deep water temperature changes derived from benthic foraminifera isotopic records. *Quat. Sci. Rev.* 21, 295–305.
- Walsh, J.P., Ridd, P.V., 2009. Processes, sediments, and stratigraphy of the Fly River Delta. In: Bolton, B.R. (Ed.), *The Fly River, Papua New Guinea: Environmental Studies in an Impacted Tropical River System. Developments in Earth and Environmental Sciences* 9, pp. 153–176.
- Walsh, J.P., Nittrouer, C.A., Palinkas, C.M., Ogston, A.S., Sternberg, R.W., Brunskill, G., 2004. Clinoform mechanics in the Gulf of Papua, New Guinea. *Cont. Shelf Res.* 24, 2487–2510.
- Wellner, R.W., Bartek, L.R., 2003. The effect of sea level, climate, and shelf physiography on the development of incised-valley complexes: a modern example from the East China Sea. *J. Sediment. Res.* 73, 926–940.
- Weltje, G.J., Brommer, M.B., 2011. Sediment-budget modelling of multi-sourced basin fills: application to recent deposits of the western Adriatic mud wedge (Italy). *Basin Res.* 23, 291–308.
- Wilson, A., Flint, S., Payenberg, T., Tohver, E., Lanci, L., 2014. Architectural styles and sedimentology of the fluvial Lower Beaufort Group, Karoo Basin, South Africa. *J. Sediment. Res.* 84, 326–348.
- Wittmer, J.M., Dexter, T., Scarponi, D., Amorosi, A., Kowalewski, M., 2014. Quantitative bathymetric models for late Quaternary transgressive-regressive cycles of the Po Plain, Italy. *J. Geol.* 122, 649–670.
- Woillard, G.M., 1978. Grand Pile peat bog: a continuous pollen record for the last 140,000 years. *Quat. Res.* 9, 1–21.
- Wright, V.P., Marriott, S.B., 1993. The sequence stratigraphy of fluvial depositional systems: the role of floodplain sediment storage. *Sediment. Geol.* 86, 203–210.